ABSTRACT

APPLICATION OF MASS/STIFFNESS ECCENTRICITY TO CONTROL RESPONSE OF STRUCTURES SUBJECTED TO EARTHQUAKE GROUND MOTION

by
Bakhtiar Feizi

This dissertation is driven by the concept that engaging more modes in the response of structures can be used to mitigate its translational dynamic response. One such an approach is to engage torsional modes through engineered eccentricity (mass/stiffness eccentricity), thus, introducing coupled translation-rotation response. This idea was first introduced in a paper published by MacBain and Spillers in 2004. As a follow up to the same idea this dissertation was an attempt to investigate and develop the theory concerning the application of mass/stiffness eccentricity to control the translational motion of structures subjected to earthquake ground motion.

Different discrete and continuous mathematical models of structures were used for this study. Discrete models are single story building and multi story building, and continuous models are shear beam and flexural beam.

Initially, the steady state behavior of eccentric structures was analyzed. This type of analysis proved to be revealing in terms of parameters that impact the response mitigation. A sufficient and necessary condition under which increasing eccentricity in a single story building always leads to mitigation of translational displacement was deducted. Moreover it was observed that in addition to the eccentricity the relationship between dominant translational frequency to dominant rotational frequency plays a significant role in the magnitude of reductions.

Furthermore through conducting a statistical analysis the seismic effectiveness of the proposed method was investigated. For this purpose the structural models were exposed to 16 real earthquake records. The records were selected in a way that a broad range of frequency content were covered. The records are applied to structures with different eccentricities and frequency ratios. Altogether 5632 analyses were performed. The results showed that eccentricity was indeed effective in reducing the average translational displacements up to 30%. Moreover, using the data obtained from time history analyses the variation of reductions with eccentricity and frequency ratio was studied.

The dissertation continued with proposing a systematic approach for finding the eccentricities and frequency ratio that lead to the maximum reduction in displacements. To address this issue an optimization problem in frequency domain was formulated. The mean square value of response was selected as the performance function. Two types of constraints including limitations on rotations and eccentricity were imposed. Kanai-Tajimi power spectral density function was used to model the ground motion. It was observed that this approach could be used to decrease the performance function up to 50%. Finally through a case study the performance of the proposed approach was compared with tuned mass dampers (TMD). The results showed that the proposed method could be as effective as TMDs. Even in some cases more reductions in displacements could be achieved.

APPLICATION OF MASS/STIFFNESS ECCENTRICITY TO CONTROL RESPONSE OF STRUCTURES SUBJECTED TO EARTHQUAKE GROUND MOTION

by
Bakhtiar Feizi

A Dissertation
Submitted to the Faculty of
New Jersey Institute of Technology
in Partial Fulfillment of the Requirements for the Degree of
Doctor of Philosophy in Civil Engineering

Department of Civil and Environmental Engineering

January 2011

APPROVAL PAGE

APPLICATION OF MASS/STIFFNESS ECCENTRICITY TO CONTROL RESPONSE OF STRUCTURES SUBJECTED TO EARTHQUAKE GROUND MOTION

Bakhtiar Feizi

Dr. M. Ala Saadeghvaziri, Dissertation Advisor — Date
Professor of Civil and Environmental Engineering, NJIT

Dr. C. T. Thomas Hsu , Committee Member — Date
Professor of Civil and Environmental Engineering, NJIT

Dr. Taha F. Marhaba, Committee Member — Date
Professor of Civil and Environmental Engineering, NJIT

Dr. Methi Wecharatana, Committee Member — Date
Professor of Civil and Environmental Engineering, NJIT

Dr. Yuxiang Xing, Committee Member — Date
Consulting Engineer, MYX Engineers LLC

BIOGRAPHICAL SKETCH

Author: Bakhtiar Feizi

Degree: Doctor of Philosophy

Date: January 2011

Undergraduate and Graduate Education:

- Doctor of Philosophy in Civil Engineering,
  New Jersey Institute of Technology, Newark, NJ, 2011

- Master of Science in Structural Engineering,
  Tarbiat Modares University, Tehran, Iran 2003

- Bachelor of Science in Civil Engineering,
  Iran University of Science and Technology, Tehran, Iran 2000

Major: Civil Engineering

Presentations and Publications:

Saadeghvaziri M. Ala, Feizi B., Kempner Jr. L., Alston D. "On Seismic Response of Substation Equipment and Application of Base-Isolation to Transformers", IEEE Transactions on Power Delivery, Vol. 25 Issue 1, pg 177-187, January 2010.

Saadeghvaziri M. Ala, Feizi B. "Beneficial Aspects of Multi-Hazard Approach to Design of Highway Bridges", 6th National Seismic Conference on Bridges & Highways, Charleston, South Carolina, July 2008.

Saadeghvaziri M. Ala, Feizi B. "On Seismic Specifications for Highway Bridges in the US", 3rd International Bridge Conference, Tehran, May 2008.

Ersoy S., Feizi B., Ashrafi A. , Saadeghvaziri M. Ala "Seismic Evaluation and Rehabilitation of Critical Electrical Power System Components" Final Technical Report, Multidisciplinary Center for Earthquake Engineering Research (MCEER), March 2008.

Feizi B., Saadeghvaziri M. Ala, Wang S., "On Modeling and Progressive Collapse of Highway Bridges Subjected to Blast Load", 1st Inter. Workshop on Performance,

Protection and Strengthening of Structures under Extreme Loading, Whistler, Canada, August 2007.

Saadeghvaziri M. Ala., Allaverdi N., L. Kempner and Feizi B. "Advantages and Considerations in Application of Base-isolation to Substation Transformers", 9th Canadian Conference on Earthquake Engineering, Quebec, Canada, June 2007.

Feizi B., Allaverdi N., "Advantages and Considerations in Application of Base-Isolation to Substation Transformers: A Case Study", Poster Presented in EERI Annual Meeting, Universal City, Los Angeles, February 2007.

To:

Shilan Motamedvaziri

ACKNOWLEDGEMENT

This dissertation was based on an idea by the late Professor William R. Spillers. I would like to express my sincere appreciation to him for his guidance and thoughtful inputs. He was a true scholar and a great gentleman. It was an honor to work with him on this dissertation.

I am deeply indebted to Professor M. Ala Saadeghvaziri, not only because of his technical advice but also for his unfailing and invaluable support over the past four years. I consider myself quite fortunate to have known him. Special thanks is given to the committee members: Professor Tom Hsu, Professor Taha Marhaba, Professor Methi Wecharatana and Dr. Michael Xing for their time, comments and instrumental cooperation. I would like to also thank Dr. Navid Allahverdi for his continuous assistance over the course of this research.

Finally, I would like to thank Department of Civil and Environmental Engineering and Office of Graduate Studies for providing financial support in pursuit of this degree.

TABLE OF CONTENTS

TABLE OF CONTENTS
(Continued)

Chapter **Page**

TABLE OF CONTENTS
(Continued)

Chapter	**Page**

LIST OF TABLES

LIST OF FIGURES

LIST OF FIGURES
(Continued)

Figure **Page**

LIST OF FIGURES
(Continued)

Figure **Page**

LIST OF FIGURES
(Continued)

Figure **Page**

CHAPTER 1

INTRODUCTION

1.1 Background Information

Due to a variety of reasons such as irregular architectural forms, asymmetric distribution of mass or stiffness in plan or complicated geometries the center of mass and stiffness (rigidity) are apart in many structures and this fact makes the existence of eccentricity inevitable. In such structures the translational displacements in two orthogonal directions and rotation can no longer be treated separately, for they are actually coupled in the governing differential equations of motion. Therefore introducing eccentricity into the vibration problems will lead to activation of rotational degree of freedom and participation of a higher number of modes in the response.

Generally speaking, rotation is considered to be undesirable by many structural engineers. There is a plethora of literature in this regard and almost everywhere the focus is on finding ways to eliminate, mitigate or accommodate the unwanted rotation. However the possibility that this irregularity could be manipulated to reduce the translational vibrations had never been investigated until a paper was published in 2004 by MacBain and Spillers.

MacBain and Spillers showed that three-dimensional effects caused by eccentricity can be used to reduce system vibrations in a dispersion-like manner (MacBain and Spillers 2004) by engaging new modes. Therefore by engineering the eccentricity and adept application of it, a new method of passive control can be developed that could lead to significant reductions in translational vibration of structures.

Thus this research is an attempt to investigate and develop the theory concerning the application of mass/stiffness eccentricity in controlling translational motion of structures subjected to base excitation.

1.2 Literature Review

An extensive amount of research has been conducted to address the dynamic and more specifically seismic response of asymmetric structures and improving torsional provisions of seismic codes. Recent reviews on this subject can be found in (De Stefano and Pintucchi 2008). The trend that is easy to see is that the researchers are trying to find the tools to mitigate the unwanted rotational displacements induced in structures due to irregularities.

Moreover, over the last two decades, a significant amount of research has been devoted to develop theories and tools to control the structural vibrations under loading conditions such as earthquake and wind. Most of the approaches implemented to control the vibrations can be divided into four categories namely: passive, active, semi active and hybrid control methods (Spencer Jr and Nagarajaiah 2003). Passive control strategies have been well understood and have been widely accepted by structural engineers in both academia and practice (Spencer Jr and Nagarajaiah 2003). Base isolation systems, tuned mass dampers and viscoelastic dampers are among the most well known passive control systems. According to the nature of passive control, the application of the eccentricity of mass/stiffness in reducing the translational vibration would belong to this category.

As it was mentioned earlier, there are plenty of literature on asymmetric structures and passive control systems, however the only literature available which is directly

related to the subject of this proposal is the paper published by MacBain and Spillers in 2004 (MacBain and Spillers 2004). All the results and analyses presented in this section are from that paper.

MacBain and Spillers have studied the behavior of a single story building subjected to a step input of base motion in x direction [$\delta_{x_0} = H(t)$]. If the eccentricities are zero the response of the system is only translational displacement in x direction ($1-\cos(\omega_x t)$). In this case the response is obviously equivalent to the response of a single degree of freedom system with H(t) at the base. However, by introducing the eccentricity in both directions, all the three degrees of freedom of the system are activated. The responses of the eccentric system with and without damping are compared in Figure 1.1.

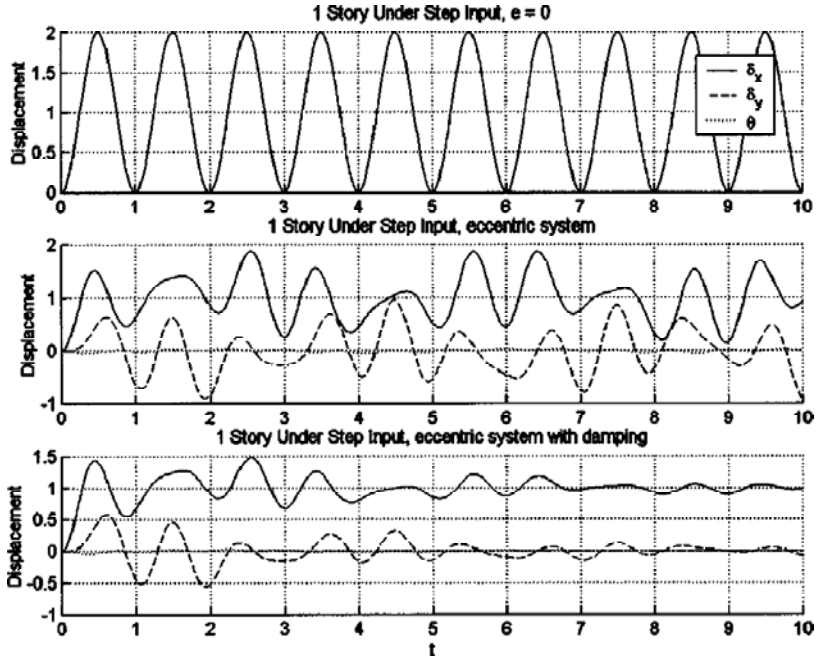

Figure 1.1 Behavior of a single story building with and without eccentricity.

Second graph of Figure 1.1 shows that eccentricity can reduce the initial displacement by about 25%. However, if the damping is not taken into account the input energy finds its way back into vibration in the *x*-direction over time and the reduction is lost. But if damping is taken into account damping would take care of the long term response (MacBain and Spillers 2004).

Additionally, it was mathematically shown that for a system with equal stiffness and eccentricity in both directions the short time solution to the translational displacement can be made smaller by increasing the eccentricity. The maximum possible reduction in the initial primary response could reach up to 50% (MacBain and Spillers 2004).

Moreover, both step function and earthquake inputs were applied to a two story building. Plots of the maximum displacement of the structure at the top floor indicate the general trend of decreasing response with increasing eccentricity (Figures 1.2 and 1.3) (MacBain and Spillers 2004).

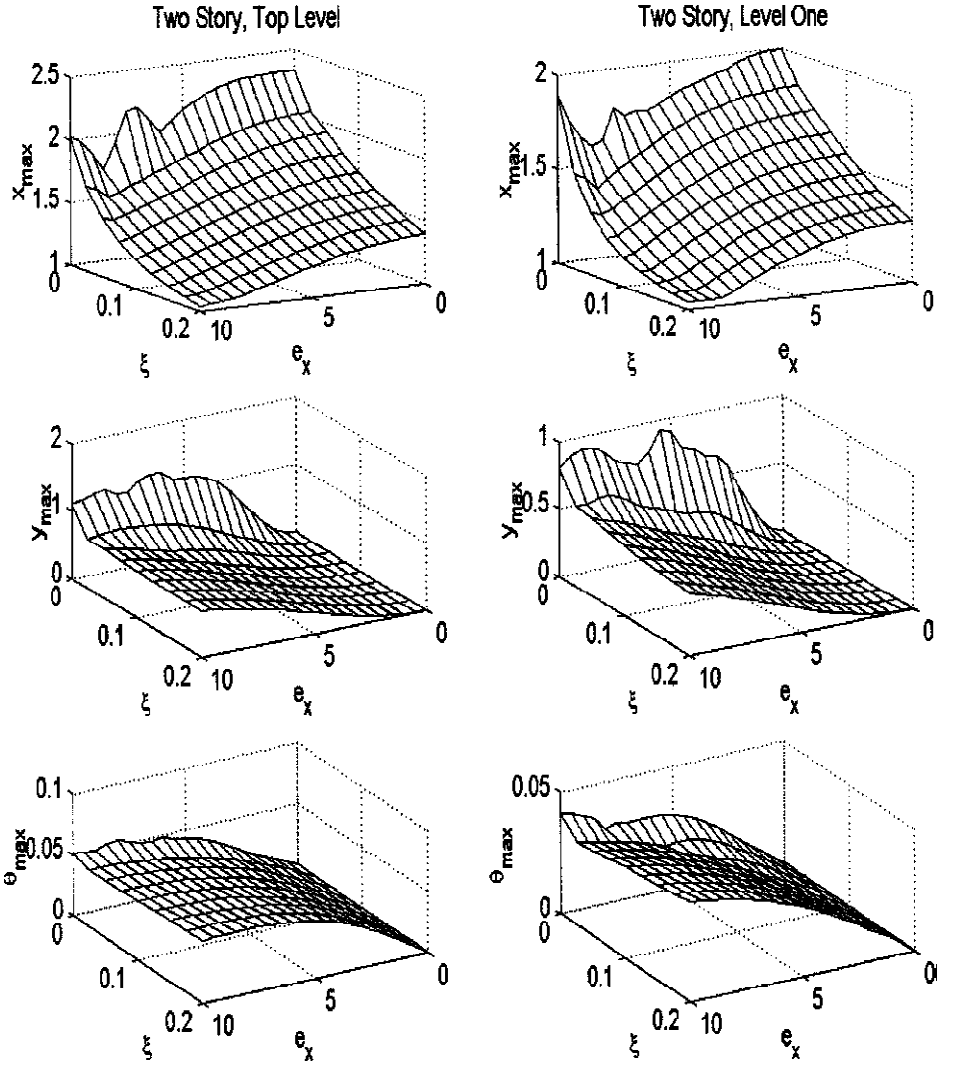

Figure 1.2 Two story response to unit-step displacement applied in x-direction.

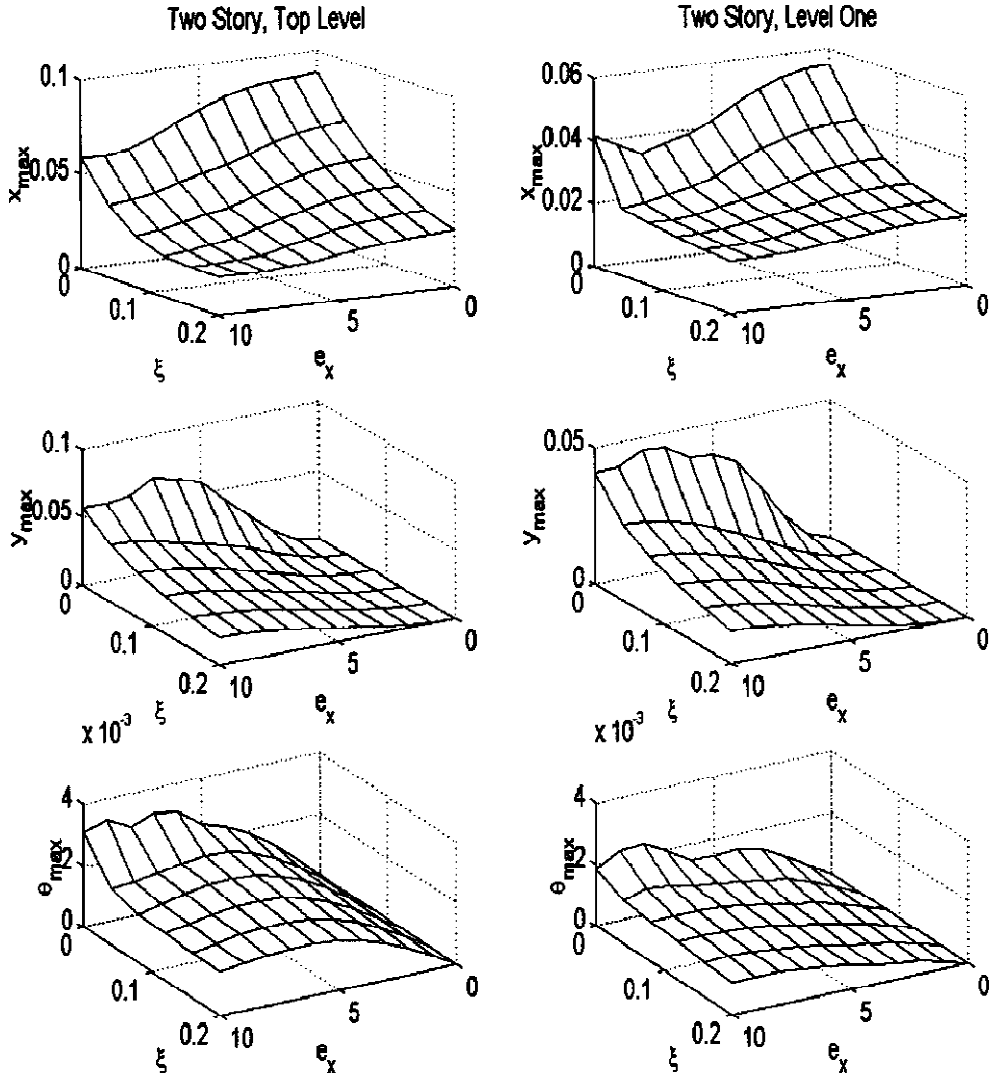

Figure 1.3 Two-story response to Parkfield earthquake record applied in x-direction.

1.3 Objective

The paper discussed in the previous section was a proof of concept. As a follow up to the same idea, the objective of this research is to develop the theory and investigate the application of mass/stiffness eccentricity in motion control of structures under base excitation. To this end the emphasis would be on two important concepts:

1. Investigating the effectiveness of the proposed passive control method for seismic loading.
2. Finding an approach to tune the eccentricity in a way that under certain circumstances the maximum amount of reduction is achieved.

To study these concepts the research is broken down into four major parts as follows:

1.3.1 Steady State Response of Structures with Mass/Stiffness Eccentricity

This first task is the starting point of this research. The approach used to do this part is almost analogous to that of tuned mass dampers (TMD). TMD in the simplest case is a new degree of freedom introduced to the structure. The frequency of this new DOF is tuned so the displacements of the main structure are controlled. Developing the theory of TMDs started with steady state analysis. Therefore, the author believes that selecting steady state analysis could be a very informative starting point as far as this research is concerned.

Four structural models are selected to represent different structural systems. These structural models are introduced in the next chapter. A harmonic load is applied to these systems and the steady state response is studied. It is expected that studying the behavior of the eccentric structures under this loading condition would be very helpful in finding the parameters that impact the response of eccentric structures.

1.3.2 Seismic Effectiveness of Eccentricity in Mitigation of Translational Response

The first part of this task deals with statistical analysis with historical earthquakes. For this purpose an ensemble of historical earthquake records are selected. They are applied to all four models with different values of translational and rotational frequency. The

eccentricity is varied uniformly over the height and the maximum reduction in translational displacement is found. By calculating some statistical parameters such as mean, median and standard deviations of reductions, the effectiveness of eccentricity in mitigation of displacements when the structure is subjected to real earthquakes is studied.

The second part is on parametric analysis of the behavior of eccentric structures under base excitation. The main objective in this part is to study the parameters that impact the amount of reduction obtained by using eccentricity as a strategy for motion control. For this purpose the structures are subjected to several earthquake records and the amount of reduction versus different parameters are analyzed and the impact of this parameters along with eccentricity is studied. The time history response of eccentric structural models will be studied as well.

1.3.3 Optimal Design of Eccentricity for Seismic Applications

Similar to the previous parts studying the optimal design of eccentricity is addressed in two subsections. The first subsection is on optimal eccentricity for a single story building. The central problem in this subsection is to solve an optimization problem that finds the maximum reduction in displacements. The state variables are eccentricity and the ratio of translational frequency to rotational frequency. There are different strategies to approach this problem, namely: using the displacement-eccentricity graphs developed in the previous task, formulating the optimization problem in frequency domain and using optimal control theory approach.

The second problem to be solved is finding the optimal variation of eccentricity over the height for a multistory system. For this section, the method opted in the previous section is used to generalize the solution to a multistory system.

1.3.4 Conducting a Case Study

The main objective of this section is comparing the performance of a renowned passive control method with the proposed strategy through conducting a case study.

1.4 Intellectual Merit

This work deals with a new phenomenon: how mass/stiffness eccentricity can be used to damp structural vibration. Its application should lead to new approaches in structural design.

CHAPTER 2

METHODOLOGY

The main focus of this chapter is to describe an overview of the methodology that is going to be used for accomplishing the tasks mentioned in the previous chapter.

It should be noted that throughout this dissertation *non-eccentric structure* wherever used, refers to the structure in which the center of mass and stiffness (rigidity) are identical, and the structure with eccentricity of mass/stiffness is simply called *eccentric structure*.

2.1 Structural Models

The structural models that have been used in the literature can be divided into two main groups: discrete and continuous.

2.1.1 Discrete Models

Two discrete models will be used in this research. The first one is a single story building (SSB) shown in Figure 2.1. This model is very popular and has been extensively used by researchers to study the irregularities in structures (De Stefano and Pintucchi 2008).

In Figure 2.1 C_M denotes the center of mass and C_s denotes the center of stiffness (rigidity). If these two points (centers) are separate the building is considered to be eccentric. It is assumed that the origin of the coordinate system is located at the center of mass. The system has three degrees of freedom (DOF), and the displacement vector which consists of two translational displacements in x and y directions and one rotation is:

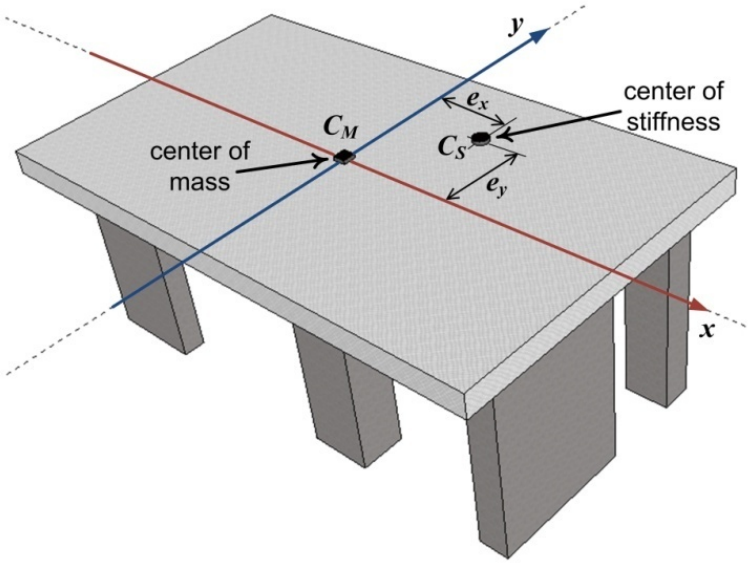

Figure 2.1 A simplified model of a single story building with eccentricity.

$$\boldsymbol{\delta}(t)=\begin{bmatrix}\delta_x(t)\\ \delta_y(t)\\ \theta(t)\end{bmatrix} \tag{2.1}$$

The dynamic equation of motion is:

$$\boldsymbol{M}\ddot{\boldsymbol{\delta}}(t)+\boldsymbol{C}\dot{\boldsymbol{\delta}}(t)+\boldsymbol{K}\boldsymbol{\delta}(t)=\boldsymbol{P}(t) \tag{2.2}$$

The matrixes of stiffness and mass for the model shown in Figure 2.1 can be expressed as (Chopra 1995) :

$$\boldsymbol{K}=\begin{bmatrix}k_x & 0 & -e_y k_x\\ 0 & k_y & e_x k_y\\ -e_y k_x & e_x k_y & k_\theta + e_y^2 k_x + e_x^2 k_y\end{bmatrix} \tag{2.3}$$

$$\boldsymbol{M}=\begin{bmatrix}m_x & 0 & 0\\ 0 & m_y & 0\\ 0 & 0 & I_O\end{bmatrix} \tag{2.4}$$

In which:

k_x and k_y : translational stiffness in x and y direction

k_θ: torsional stiffness

e_x and e_y: the distance between the center of stiffness (rigidity) and y and x axes

m_x and m_y: mass of the floor in x and y direction

I_o: mass moment of inertia of the floor slab

Due to the simplicity of this model, in some particular cases, problem formulation and also obtaining the exact mathematical solution is straight forward. From the closed form solutions most of the characteristics of the response can be studied and interpreted.

The second discrete model is a multistory building (MSB) which is basically a stack of several single story buildings.

2.1.2 Continuum Models

Continuum models have also been used extensively to estimate deformations and forces in buildings subjected to wind and earthquake loads. Usually the type of deformation of a building falls into one of the following three categories (see Figure 2.2):

1. Flexural type deformation
2. Shear type deformation
3. Combined flexural and shear type deformation

For the purpose of this research, a cantilever shear beam (SBM) and a flexural beam (FBM) have been selected to model the shear type and flexural type deformations of structures respectively. It can be proven that the equation governing the vibrations of flexural beam and shear beam with eccentricities are three coupled partial differential equations (PDE).

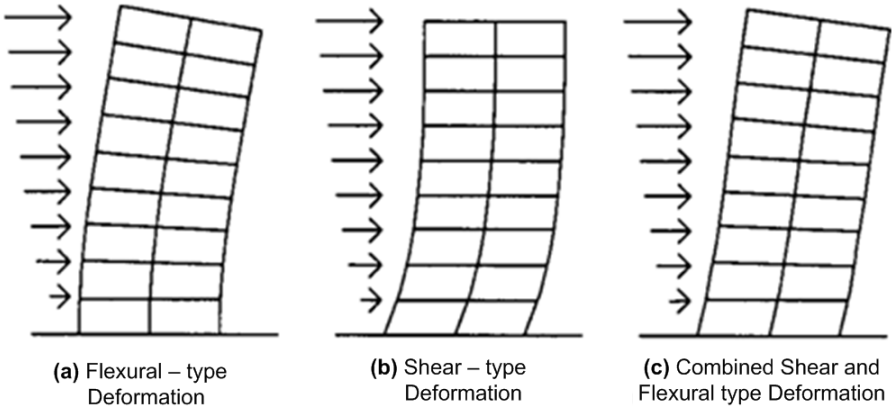

Figure 2.2 Types of deformations in building structures (Miranda et al. 2005)

The system of PDEs governing the vibration of a cantilever flexural beam can be expressed as follows:

$$\begin{cases} -\dfrac{\partial^2}{\partial z^2}\left(EI_x(z)\dfrac{\partial^2}{\partial z^2}\left(\delta_x - e_y\theta\right)\right) = m(z)\dfrac{\partial^2\delta_x}{\partial t^2} - P_x\left(z,t\right) \\ -\dfrac{\partial^2}{\partial z^2}\left(EI_y(z)\dfrac{\partial^2}{\partial z^2}\left(\delta_y + e_x\theta\right)\right) = m(z)\dfrac{\partial^2\delta_y}{\partial t^2} - P_y\left(z,t\right) \\ -\dfrac{\partial^2}{\partial z^2}\left(EI_y(z)\dfrac{\partial^2}{\partial z^2}\left(\delta_y + e_x\theta\right)\right)e_x + \dfrac{\partial^2}{\partial z^2}\left(EI_x(z)\dfrac{\partial^2}{\partial z^2}\left(\delta_x - e_y\theta\right)\right)e_y \\ \qquad + \dfrac{\partial}{\partial z}\left(GJ(z)\dfrac{\partial\theta}{\partial z}\right) = I_o(z)\dfrac{\partial^2\theta}{\partial t^2} - T\left(z,t\right) \end{cases} \tag{2.5}$$

Where:

z: vertical axis which is zero at the base of the beam and passes through the center of mass

E: modulus of elasticity,

G: shear modulus of elasticity,

I_x and I_y : moment of inertia about y and x axis

J : polar moment of inertia of the cross section

m: mass of the unit length of the beam

I_o: mass moment of inertia of the beam cross section about z-axis

P_x and P_y: distributed load in x- and y-direction

T: distributed torsion.

In addition to that the system of PDEs governing the vibration of a cantilever shear beam is expressed as:

$$\begin{cases} \dfrac{\partial}{\partial z}\left(GA(z)\dfrac{\partial}{\partial z}\left(\delta_x - e_y\theta\right)\right) = m(z)\dfrac{\partial^2\delta_x}{\partial t^2} - P_x(z,t) \\ \dfrac{\partial}{\partial z}\left(GA(z)\dfrac{\partial}{\partial z}\left(\delta_y + e_x\theta\right)\right) = m(z)\dfrac{\partial^2\delta_y}{\partial t^2} - P_y(z,t) \\ \dfrac{\partial}{\partial z}\left(GA(z)\dfrac{\partial}{\partial z}\left(\delta_x - e_y\theta\right)\right)e_y + \dfrac{\partial}{\partial z}\left(GA(z)\dfrac{\partial}{\partial z}\left(\delta_y + e_x\theta\right)\right)e_x \\ \qquad + \dfrac{\partial}{\partial z}\left(GJ(z)\dfrac{\partial\theta}{\partial z}\right) = I_o(z)\dfrac{\partial^2\theta}{\partial t^2} - T(z,t) \end{cases} \tag{2.6}$$

where

z : vertical axis

A: cross-section area

G: shear modulus of elasticity

m: mass of unit length

$\lambda = J/A$

J : polar moment of inertia for the beam

P_x and P_y: distributed load applied in x and y direction

T: torsion.

The equations governing the vibration of the flexural beam are fourth order parabolic PDEs. The equations governing the vibration of the shear beam are second order hyperbolic PDEs which are in the same category of PDEs as wave propagation problems.

2.1.3 Solution to Mathematical Models

For some particular cases, the shear beam equations can be solved analytically (Abrate 1995; Li 2002). However, finding the closed form solution for the general case for both systems is extremely difficult if not impossible. Therefore, for the purpose of this thesis, the above PDEs have been solved numerically. Some specific cases for which exact solutions are available have been used to verify the results of numerical solutions.

For solution of hyperbolic and parabolic PDEs there are several numerical schemes available in the literature. However, because of the variable stiffness and eccentricity parameters, the numbers of numerical schemes which can solve the above equations are not many. After trying a couple of methods it was observed that a combination of Finite Difference Method and Newmark time integration provides a robust and stable scheme to solve both systems. Using the finite difference method (FDM) the space (length of the beam) is discretized into several elements. This reduces the partial differential equations to a system of ordinary differential equations (ODE). In the system of ODEs the independent variable is time and using the Newmark time integration method the solutions for the displacements can be obtained.

2.2 Computer Programming

In order to solve the above mentioned systems of PDEs numerically, several object oriented computer programs have been developed in MATLAB. All the programs as well as robustness of numerical schemes have been verified.

CHAPTER 3

STEADY STATE RESPONSE OF STRUCUTRES WITH MASS/STIFFNESS ECCENTRICITY

3.1 Background Information

The main objective of this chapter is studying the steady state response of eccentric structures to harmonic loading. The approach used to address the issue is almost analogues to that of tuned mass dampers (TMD). Four cases are studied here. Analyses start with the classic single story building. Due to the simplicity of this model, problem formulation and also obtaining the exact mathematical solution is easy. It will be shown that these characteristics can be seen in more complicated cases too. Then, a multi-story building which is a stack of several single story buildings is studied. The chapter continues with studying the behaviors of flexural and shear beam. For each case numerical examples will be presented.

3.2 Single Story Building

The classic single story building (Figure 2.1) is basically a rigid floor with three degrees of freedom. The degrees of freedom are translational displacements in x- and y- direction plus rotation. This system has been extensively used in the literature. As it can be seen in Figure 2.1 the eccentricity can exist in two directions. If this is the case a load applied in x or y direction would lead to activation of all three degrees of freedom. Therefore, the equations of motions are the three coupled equations introduced in Equations (2.1) to (2.4).

However, in this section, for the sake of simplicity it is assumed that the plan is eccentric only in y-direction. In this case if the load is applied in x direction there will be no displacement in y direction for the system is symmetric with respect to y-axis, thus just two degrees of freedom will be activated (Figure 3.1) and the equations of motion for the plan shown in Figure 3.1 would reduce to two coupled equations.

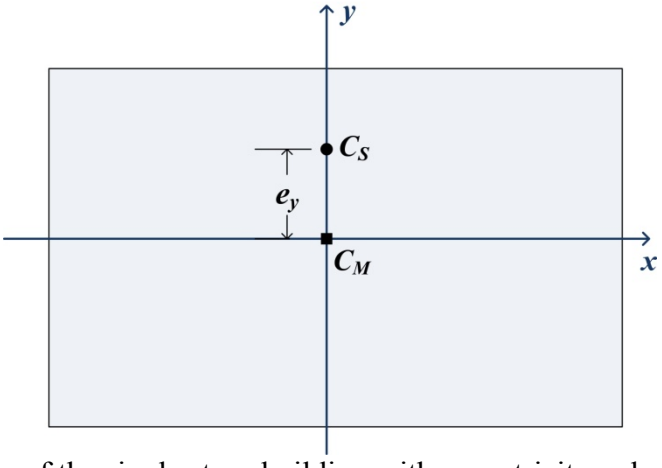

Figure 3.1 Plan of the single story building with eccentricity only in y-direction.

If the load applied to the structure is a harmonic load as:

$$\boldsymbol{P}(t) = \boldsymbol{P}_0 \sin(\Omega t) = \begin{bmatrix} P_{x_0} \\ 0 \end{bmatrix} \sin(\Omega t) \tag{3.1}$$

the steady state responses at the *center of mass* would be a displacement in x-direction and a rotation about the vertical axis:

$$\boldsymbol{\delta}(t) = \boldsymbol{\delta}_0 \sin(\Omega t) = \begin{bmatrix} \delta_{x_0} \\ \theta_0 \end{bmatrix} sin(\Omega t) \tag{3.2}$$

Since the positive direction of rotation is considered to be counterclockwise, the displacement of the *center of stiffness (rigidity)* in x-direction can be written as:

$$\delta_x^* = \delta_x - e_y \theta \tag{3.3}$$

Now by substituting Equations (3.1) and (3.2) in Equation (2.2) we will have:

$$\left(\boldsymbol{K}-\Omega^2\mathbf{M}\right)\delta_0=\mathbf{P}_0 \tag{3.4}$$

Thus:

$$\delta_0=(\mathbf{K}-\Omega^2\ \mathbf{M})^{-1}\mathbf{P}_0 \tag{3.5}$$

From the above equation, the solutions of δ_{x_0} and θ_0 will turn out to be:

$$\delta_{x_0}=\frac{P_{x_0}}{K_x}.\frac{\gamma_x\left[(\gamma_\theta-1)+\alpha\gamma_x e_y^2\right]}{(\gamma_\theta-1)(\gamma_x-1)-\alpha\gamma_x e_y^2} \tag{3.6}$$

$$\theta_0=\frac{P_{x_0}e_y}{K_\theta}.\frac{\gamma_x\ \gamma_\theta}{(\gamma_\theta-1)(\gamma_x-1)-\alpha\gamma_x e_y^2} \tag{3.7}$$

where:

$$\gamma_x=\frac{\omega_x^2}{\Omega^2}\quad,\quad \gamma_\theta=\frac{\omega_\theta^2}{\Omega^2}\quad,\quad \alpha=\frac{M}{I_o} \tag{3.8}$$

and also :

$$\omega_x^2=\frac{K_x}{M}\qquad and\qquad \omega_\theta^2=\frac{K_\theta}{I_o} \tag{3.9}$$

It is easy to see that ω_x and ω_θ are the translational and rotational frequency of the non-eccentric structure and γ_x and γ_θ are the ration of these two parameters to the load frequency.

And now in order to study the effect of eccentricity on the translational response of the structure a new parameter is defined as follows:

$$R_x=\frac{\delta_{x_0}}{\bar{\delta}_{x_0}} \tag{3.10}$$

where $\bar{\delta}_{x_0}\ sin(\Omega t)$ is the response of the primary structure to the harmonic load of Equation (3.1). It is known from classical structural dynamics that:

$$\bar{\delta}_{x_0} = \frac{\gamma_x}{\gamma_x - 1} . \frac{P_{x_0}}{K_x} \tag{3.11}$$

Therefore, by substituting Equations (3.6) and (3.11) in (3.10) R_x would become:

$$R_x = \frac{(\gamma_x - 1)\left[(\gamma_\theta - 1) + \alpha\gamma_x e_y^2\right]}{(\gamma_\theta - 1)(\gamma_x - 1) - \alpha\gamma_x e_y^2} \tag{3.12}$$

Basically R_x is the ratio of the translational displacement of the eccentric structure to that of the non-eccentric structure and shows how applying eccentricity can impact the steady state response of the non-eccentric structure. If $R_x < 1$ then it shows that application of eccentricity has reduced the displacement.

As it can be seen from Equation (3.12), R_x is a function of the load frequency (Ω^2), ω_x^2, ω_θ^2, shape of the floor slab (α) and eccentricity (e_y). In addition to R_x it is important to define another parameter to study the changes in rotation with eccentricity. For this purpose Equation (3.7) is divided by P_{x_0} / K_θ and a new parameter named S_θ is introduced as follows:

$$S_\theta = \frac{\gamma_x \gamma_\theta e_y}{(\gamma_\theta - 1)(\gamma_x - 1) - \alpha\gamma_x e_y^2} \tag{3.13}$$

Now from Equation (3.12) the circumstance under which increasing eccentricity reduces the translational response can be found. The argument could be put this way: since all the parameters in Equation (3.12) are positive then if

$$(\gamma_\theta - 1)(\gamma_x - 1) < 0 \tag{3.14}$$

the absolute value of the denominator of Equation (3.12) would increase with increasing the eccentricity and consequently R_x reduces as an indication that the translational

displacement is getting smaller. On the other hand if the condition in (3.14) is not satisfied, R_x starts to increase by increasing the eccentricity until the eccentricity reaches its critical value. *Critical eccentricity* is the eccentricity for which the response of the structure is infinity as an indication that the system is undergoing resonance. The value of critical eccentricity can be calculated by setting the denominator of Equation (3.12) to zero:

$$e_{y_{cr}} = \frac{(\gamma_\theta - 1)(\gamma_x - 1)}{\alpha \gamma_x} \tag{3.15}$$

It is beyond this point that R_x starts to decrease.

Therefore, Equation (3.14) is the *sufficient and necessary* condition under which increasing eccentricity *always* mitigates the translational response in a single story building.

Another case that is interesting to study is when $\gamma_\theta = 1$. By substituting this value for γ_θ in Equations (3.6), (3.7), (3.3), (3.12) and (3.13) we have:

$$\delta_{x_0} = -\frac{P_{x_0}}{\alpha K_\theta} \tag{3.16}$$

$$\theta_0 = -\frac{P_{x_0}}{\alpha K_\theta e_y} \tag{3.17}$$

$$\delta_x^* = 0 \tag{3.18}$$

$$R_x = 1 - \gamma_x \tag{3.19}$$

$$S_\theta = -\frac{1}{\alpha e_y} \tag{3.20}$$

The above equations indicate that when $\gamma_\theta = 1$ the responses are not dependent on translational stiffness and the displacement of center of stiffness (rigidity) is actually

zero. Moreover the displacement of the center of mass is remained unchanged with changing eccentricity.

What happens in this case is a state of pure rotation about the center of stiffness (rigidity). Since δ_x and $-e_y\theta$ are equal and anti-phase, they cancel out each other at the center of stiffness (rigidity). Since the displacement of the center of stiffness (rigidity) becomes zero, the translational stiffness of structure does not contribute in the response.

On the other hand, the value of rotation is a function of eccentricity. By increasing the eccentricity the rotation decreases. It is interesting that the steady response of different single-story buildings with the same rotational stiffness and eccentricity is identical in this case. However, it should be noted that to avoid resonance, the natural frequencies of the structure has to be far enough from ω_θ . It can be seen that eccentricity is a critical parameter in controlling the rotation in this case.

In an effort to better understand the behavior of the single story building model an example has been solved. A single story building with a square shape plan is assumed. The floor is 24m wide and 0.15m thick. The mass density of the floor material is 2350 Kg/m^3. By changing the translational and rotational stiffness different values of γ_x and γ_θ have been generated and finally for different values of γ_x and γ_θ the graphs depicting the absolute values of R_x and S_θ vs. eccentricity have been plotted. The plots are presented in Figure 3.2 through Figure 3.7.

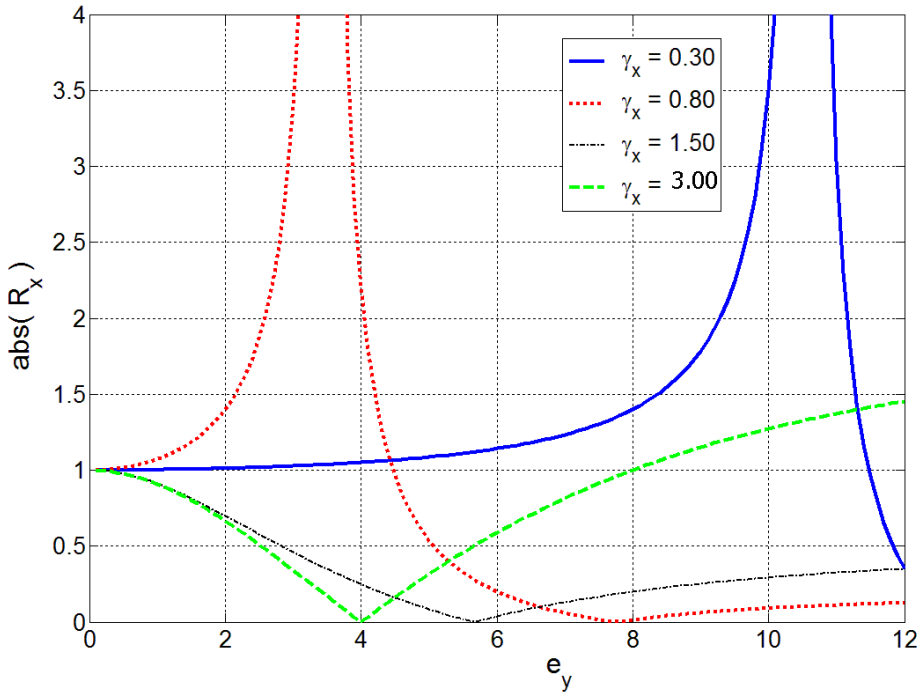

Figure 3.2 Variation of R_x with eccentricity for a single story building ($\gamma_\theta = 0.50$) .

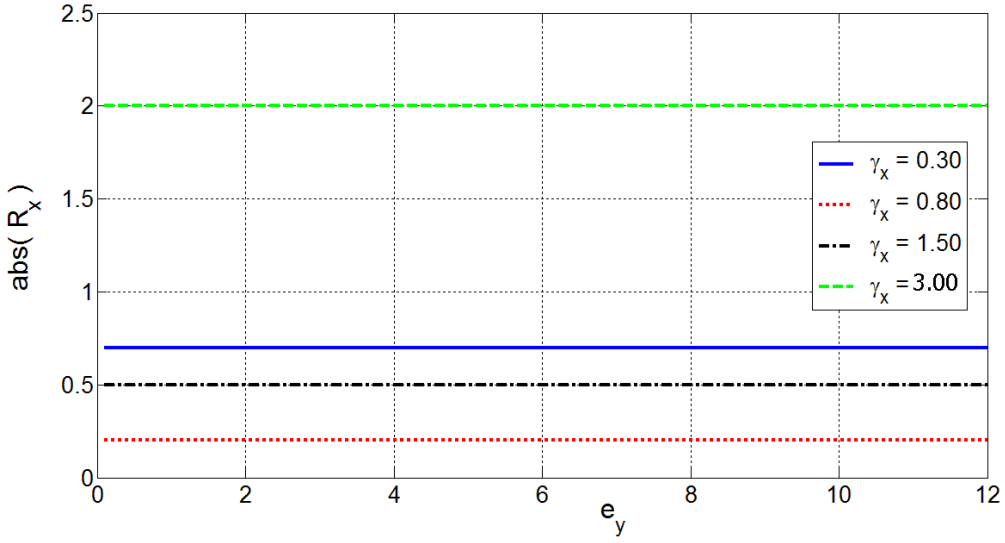

Figure 3.3 Variation of R_x with eccentricity for a single story building ($\gamma_\theta = 1.00$) .

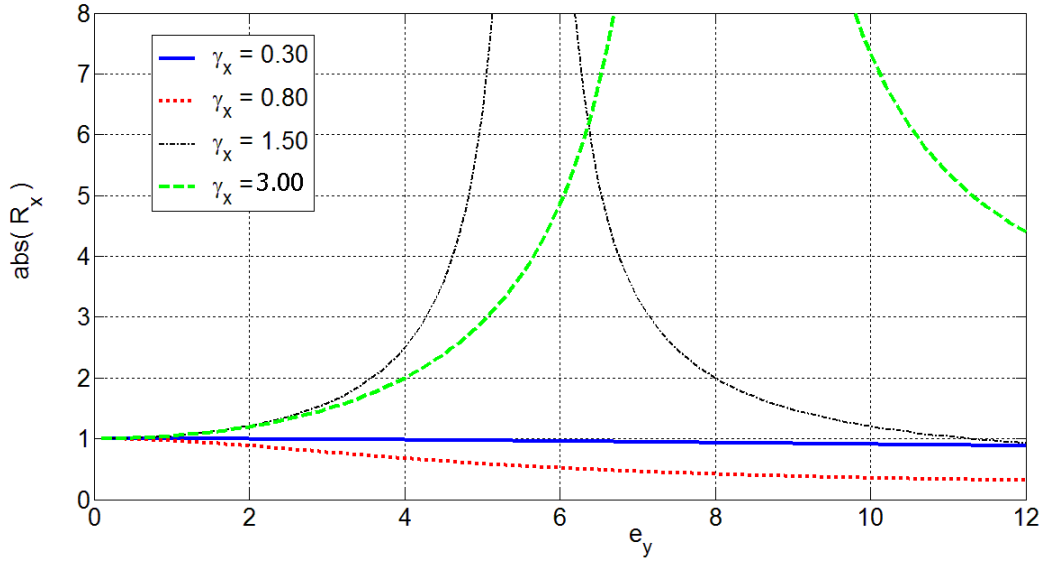

Figure 3.4 Variation of R_x with eccentricity for a single story building ($\gamma_\theta = 2.00$).

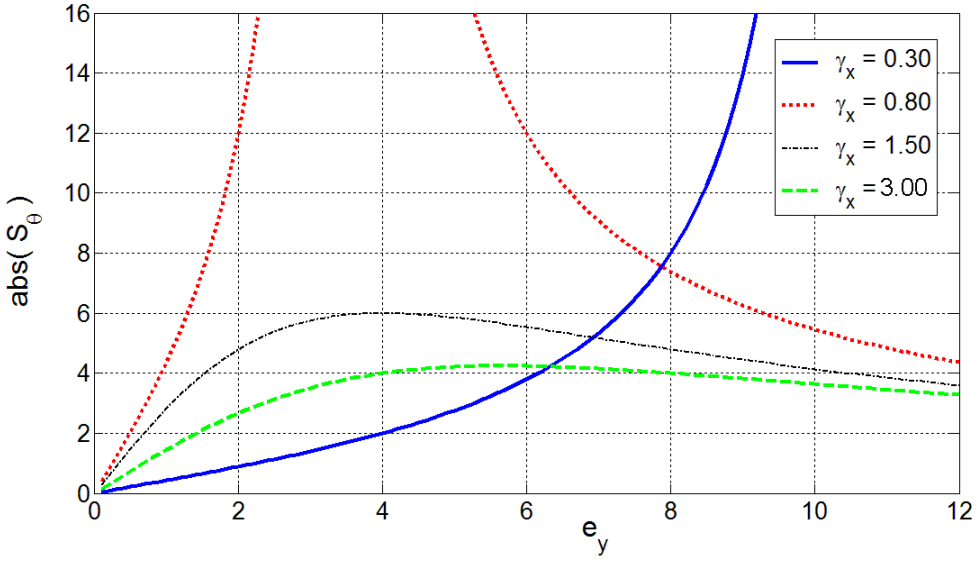

Figure 3.5 Variation of S_θ with eccentricity for a single story building ($\gamma_\theta = 0.50$).

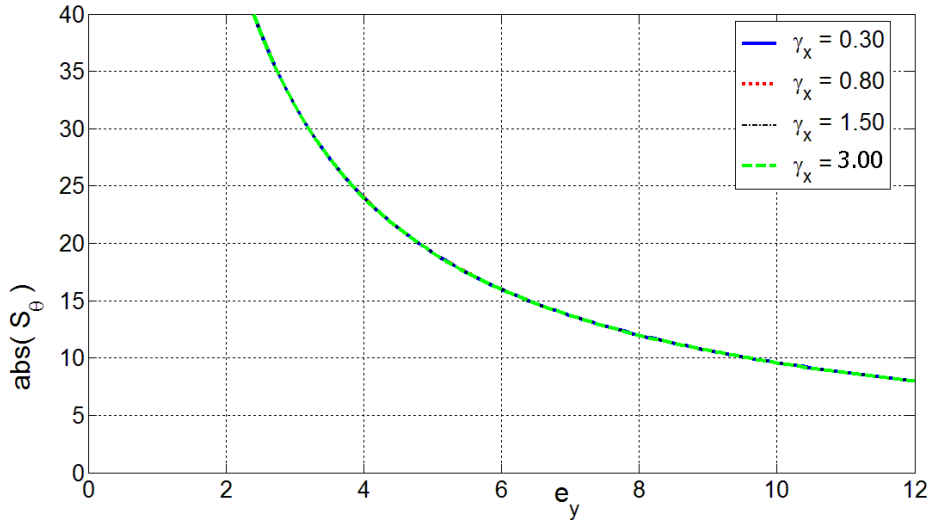

Figure 3.6 Variation of S_θ with eccentricity for a single story building ($\gamma_\theta = 1.00$).

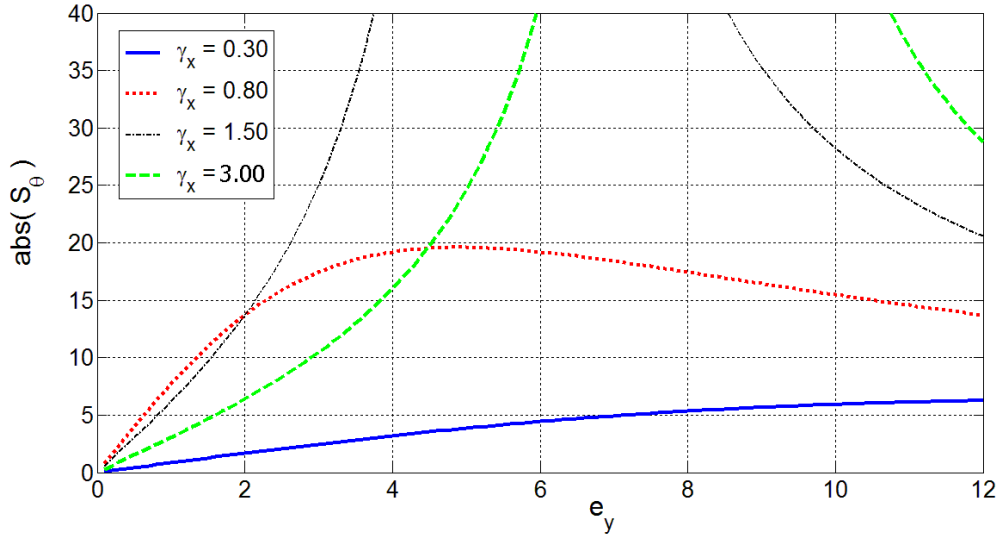

Figure 3.7 Variation of S_θ with eccentricity for a single story building ($\gamma_\theta = 2.00$).

In all the graphs shown in the figures above, except for Figures (3.3) and (3.6) which are a special case ($\gamma_\theta = 1.00$), two different types of behavior is distinguishable. In Figures (3.2) and (3.4), considering the values of γ_x and γ_θ if the condition of Equation (3.14) is satisfied then increasing eccentricity reduces the response. This is especially true in Figure (3.2) that there are eccentricities for which the response is actually zero. On the

other hand if the condition of Equation (3.14) is not satisfied then, as it was discussed earlier, the translational response starts to increase until the resonance occurs at the critical eccentricity. It is after this point that the response start to plunge. The same trends can be seen in Figures (3.5) and (3.7) too. However, in these figures if Equation (3.14) is satisfied the rotations start to increase and then after reaching a maximum they start to decrease.

It is easy to see that graphs of Figures (3.3) and (3.6) are showing an exceptional behavior. In this special case as long as γ_x is smaller than 2, eccentricity reduces the response. Moreover R_x is constant for any value of eccentricity (Equation (3.19)). Meanwhile Figure 3.6 shows that if the eccentricity is small the rotational frequency of the eccentric structure is very close to that of primary structure and since $\gamma_\theta = 1.00$, the resonance occurs. Therefore, if $\gamma_\theta = 1.00$, R_x is controlled by γ_x. That means the value of R_x is basically based on γ_x and varying the eccentricity would not change it. However, in this case eccentricity would control the rotational response.

3.3 Multi-Story Building

The multi-story building studied in this paper is basically a stack-up of eight single story buildings. Thus this model will have 24 modes of vibration. The mass and stiffness of each story is equal. The definitions of the parameters are the same and ω_x and ω_θ used here are respectively the first translational and rotational frequencies of the primary structure. In the multi-story building it is assumed that equal eccentricities are applied in both x- and y-directions. Moreover, *n* harmonic loads similar to Equation (3.1) are applied at each floor in x-direction. Just like the single story building the steady state

response is going to be sinusoidal and eventually Equations (3.4) and (3.5) are the governing equations to be solved. However, for a multi-story building **M** and **K** are $3n\times3n$ matrices and n is the number of stories. As it was mentioned earlier for the example solved in this section n=8.

Since applying an equal eccentricity to all the stories is more practical, for the rest of this section it is assumed that the value used for eccentricities at each floor is the same and equal at both directions. The objective is to study the top floor displacement of the eight-story building. For this purpose, similar to single story building, in Figures 3.8 to 3.13 the variations of R_x and S_θ versus eccentricity for top floor are presented.

Figures 3.8 to 3.10 show almost the same behavioral trend as that of Figures 3.2 to 3.4. Figure 3.8 is very similar to Figure 3.2. Figure 3.9 shows that when $\gamma_\theta = 1.00$, although the variation of R_x with eccentricity is not exactly zero, it is small enough to be negligible. Moreover in three out of the four cases the translational response of the eccentric structure is lower than non-eccentric structure, especially for the cases with $\gamma_x = 1.5$ and $\gamma_x = 0.80$. The reduction in response in these two cases is more than 80% which is significant.

There is a considerable difference between single-story and eight-story building when $\gamma_\theta = 2.00$. The difference can be seen in Figure 3.10 for the case in which $\gamma_x = 0.30$. Therefore, the statement that for a specific loading frequency resonance can be totally avoided if Equation (3.14) is satisfied is not necessarily applicable for multi-story buildings. A modal analysis of the building with $\gamma_x = 0.30$ showed that the resonance is actually due to the second mode, the frequency of which is very close to the

loading frequency. However, it is observed that when Equation (3.14) is satisfied the translational displacement, just like single story building, starts to decrease with increasing the eccentricity and when that condition is not satisfied it starts to increase with increasing the eccentricity.

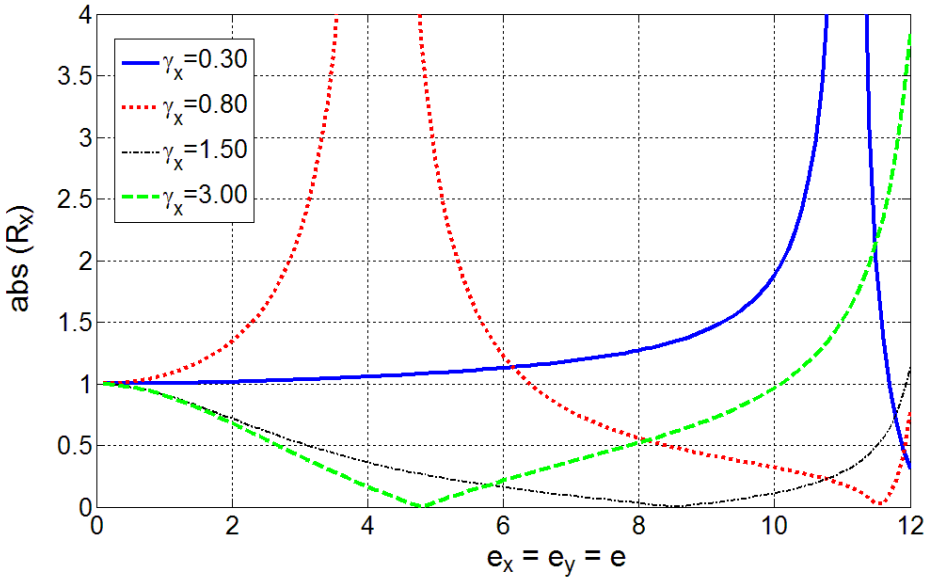

Figure 3.8 Variation of R_x at the top floor for an eight-story building with eccentricity in both directions ($\gamma_\theta = 0.50$).

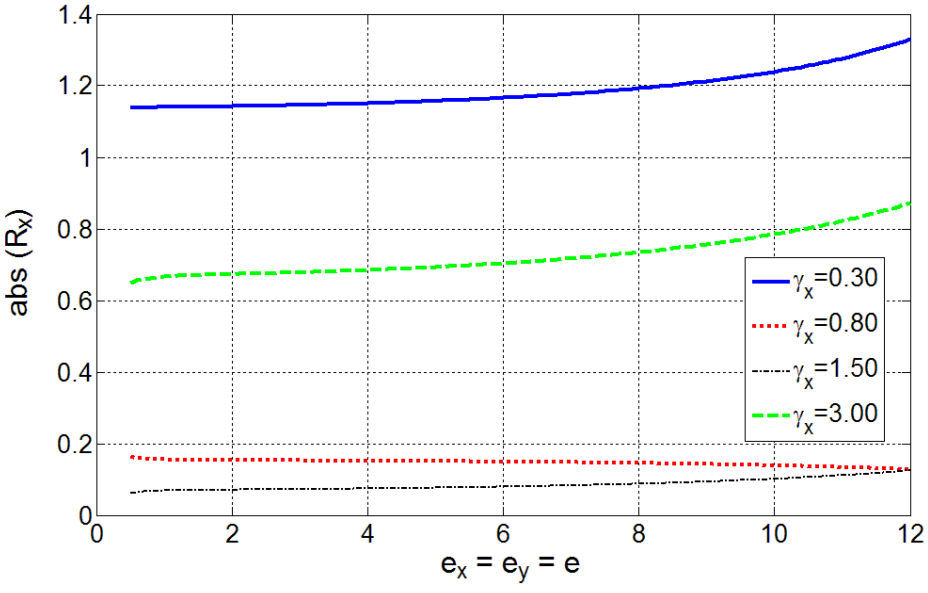

Figure 3.9 Variation of R_x at the top floor for an eight-story building with eccentricity in both directions ($\gamma_\theta = 1.00$).

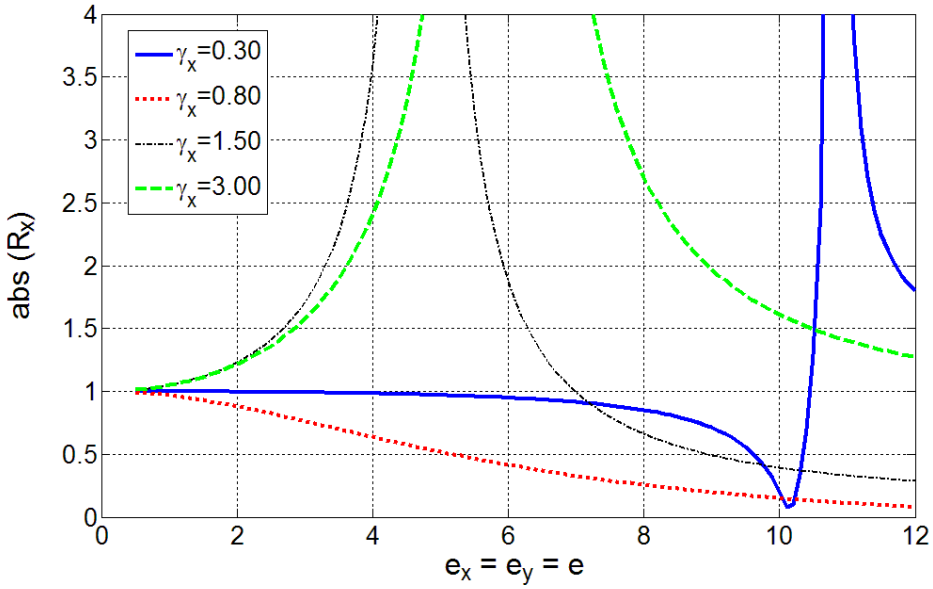

Figure 3.10 Variation of $\boldsymbol{R_x}$ at the top floor for an eight-story building with eccentricity in both directions ($\gamma_\theta = 2.00$).

In addition to R_x the variations of S_θ have been plotted. These plots are shown in Figures 3.11 to 3.13. The variations of S_θ in these figures are almost like variations of S_θ for the single story building. The difference pointed out earlier for R_x in Figure 3.8 can be seen here too. However, the insensitivity to translational stiffness observed in Figure 3.6 is not seen any more for multi story building. From Figure 3.12 it is seen that although all the structures with different translational stiffness have the same behavior, the amount of torsional response is different for each of them.

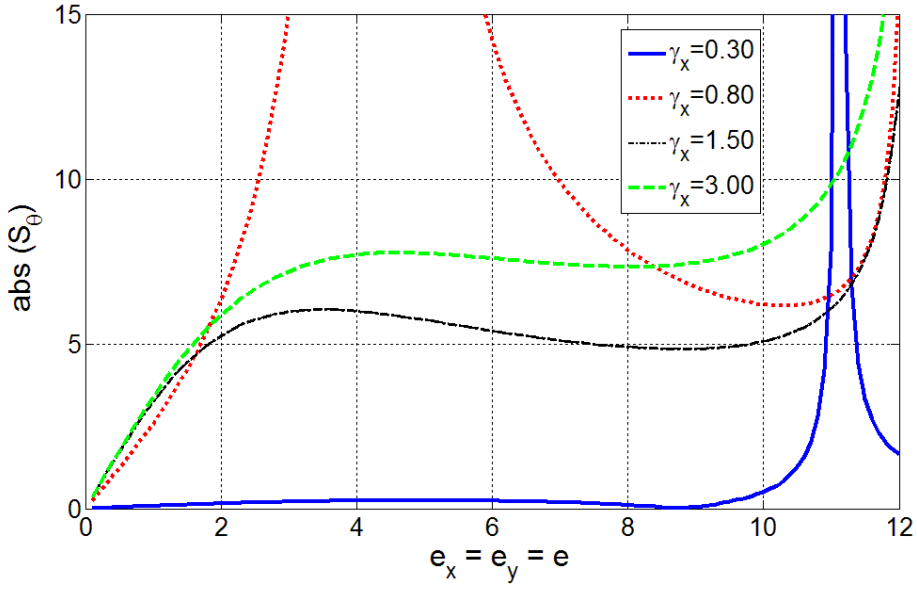

Figure 3.11 Variation of S_θ at the top floor for an eight-story building with eccentricity in both directions($\gamma_\theta = 0.50$).

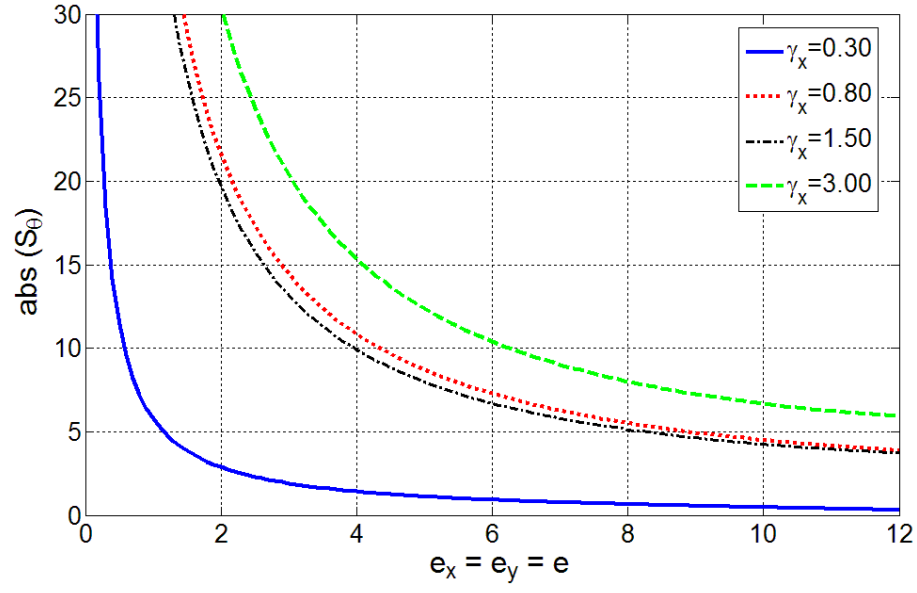

Figure 3.12 Variation of S_θ at the top floor for an eight-story building with eccentricity in both directions ($\gamma_\theta = 1.00$).

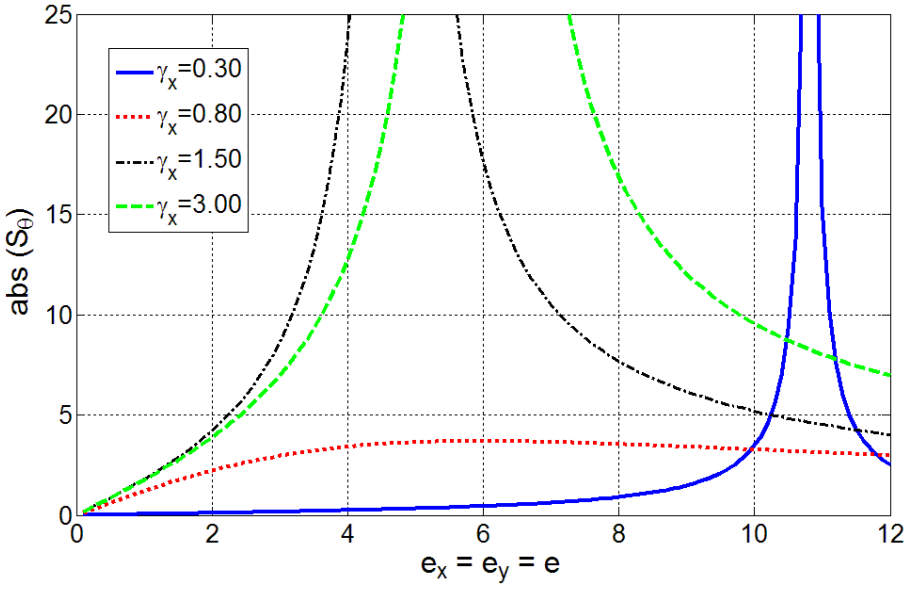

Figure 3.13 Variation of S_θ at the top floor for an eight-story building with eccentricity in both directions ($\gamma_\theta = 2.00$).

3.4 Flexural Beam Model

In order to better understand the behavior of structures with eccentricity, two continuous models have been selected for further study: flexural and shear beam. In this section, the focus will be on the flexural beam and the shear beam analysis will be discussed in the next section.

It can be proven that the equations governing the vibration of a flexural beam with eccentricity are three coupled partial differential equations (PDEs). If it is assumed that the moment of inertia, mass and eccentricity is constant over the length of the beam, the system of coupled PDEs of (2.5) can be expressed as follows:

$$\begin{cases} -EI_x\left(\dfrac{\partial^4\delta_x}{\partial z^4}-e_y\dfrac{\partial^4\theta}{\partial z^4}\right)=m\dfrac{\partial^2\delta_x}{\partial t^2}-P_x(z,t) \\ -EI_y\left(\dfrac{\partial^4\delta_y}{\partial z^4}+e_x\dfrac{\partial^4\theta}{\partial z^4}\right)=m\dfrac{\partial^2\delta_y}{\partial t^2}-P_y(z,t) \\ -EI_y\left(\dfrac{\partial^4\delta_y}{\partial z^4}+e_x\dfrac{\partial^4\theta}{\partial z^4}\right)e_x+EI_x\left(\dfrac{\partial^4\delta_x}{\partial z^4}-e_y\dfrac{\partial^4\theta}{\partial z^4}\right)e_y \\ GJ\dfrac{\partial^2\theta}{\partial z^2}=I_o\dfrac{\partial^2\theta}{\partial t^2}-T(z,t) \end{cases} \tag{3.21}$$

These equations are a set of fourth order parabolic partial differential equations. The beam is assumed to be fixed at the base and free at the other end. As it was mentioned in Chapter 2 the system of Equations (3.21) are solved numerically.

It should be noted that in this thesis Equations (3.21) are solved in normalized space. It is assumed that eccentricities are equal in both directions. A distributed harmonic load is applied in x-direction. γ_x and γ_θ are the ratios of dominant (first) translational and torsional frequencies to the load frequency. By changing the normalized eccentricities from zero to one, variations of R_x and S_θ versus eccentricity have been plotted and the corresponding graphs are presented in Figures 3.14 to 3.19.

The trends seen in these figures are more or less similar to the previous two sections, showing that the flexural beam model is having almost similar behavior to the single and multi-story building. The most significant difference is seen in Figure 3.14. For the case of $\gamma_x = 0.30$ the critical eccentricity is larger than one and is practically larger than the feasible eccentricity. This is the reason why for this case the resonance cannot be seen while for single and multi-story buildings the critical frequency happens

to be within the range of plotted eccentricities. The same discussion applies to Figure 3.17.

Additionally, Figure 3.15 shows that the translational response of all the eccentric structures are smaller than that of non-eccentric structures. The reduction varies from about 10% to 70%.

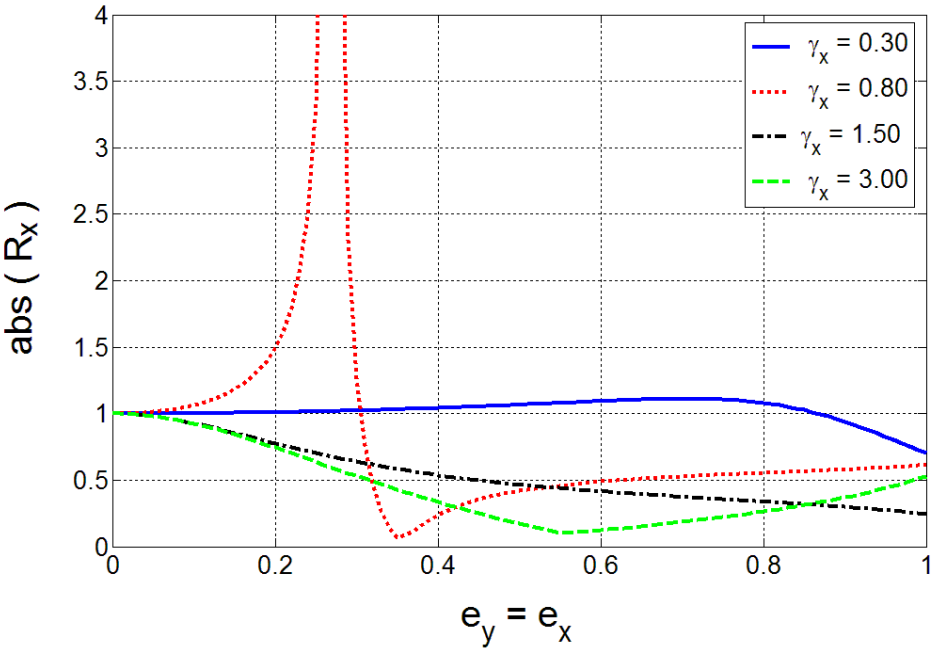

Figure 3.14 Variation of $\boldsymbol{R_x}$ at the top of the flexural beam with eccentricity in both directions ($\gamma_\theta = 0.50$).

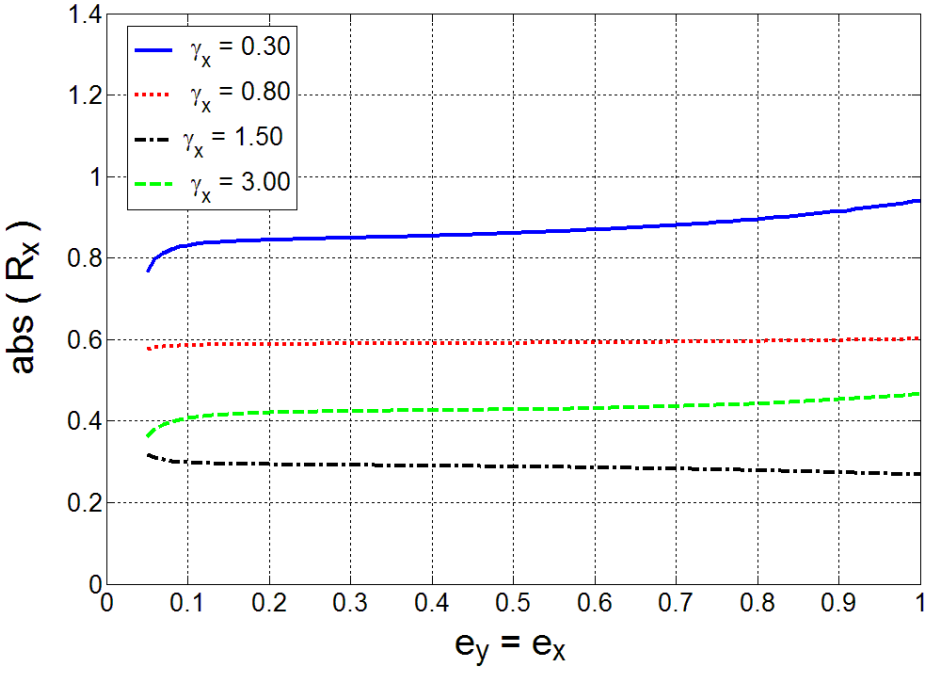

Figure 3.15 Variation of R_x at the top of the flexural beam with eccentricity in both directions ($\gamma_\theta = 1.00$).

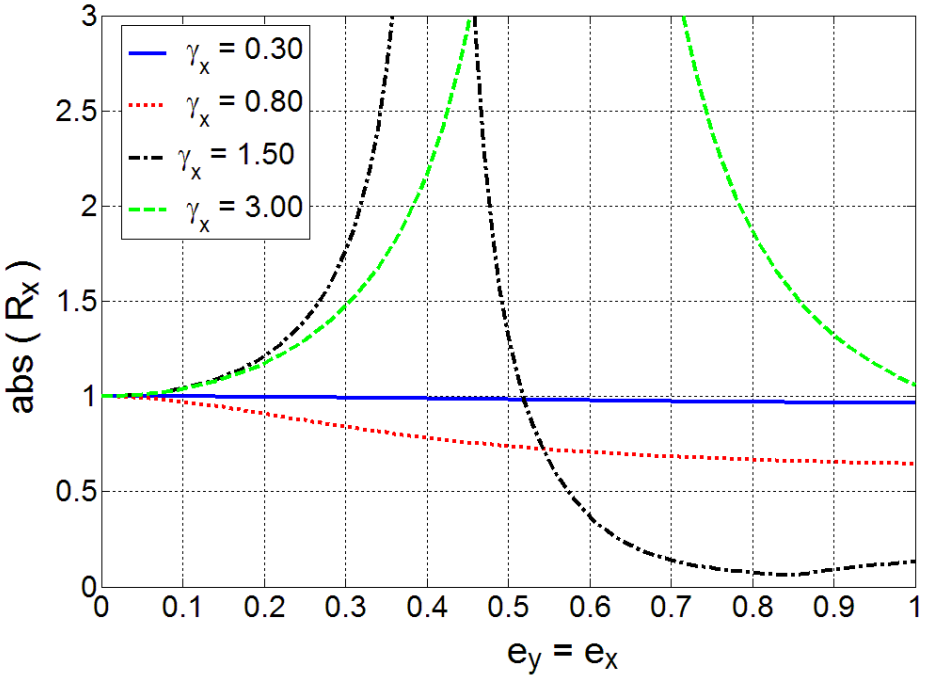

Figure 3.16 Variation of R_x at the top of a shear bean with eccentricity in both directions ($\gamma_\theta = 2.00$).

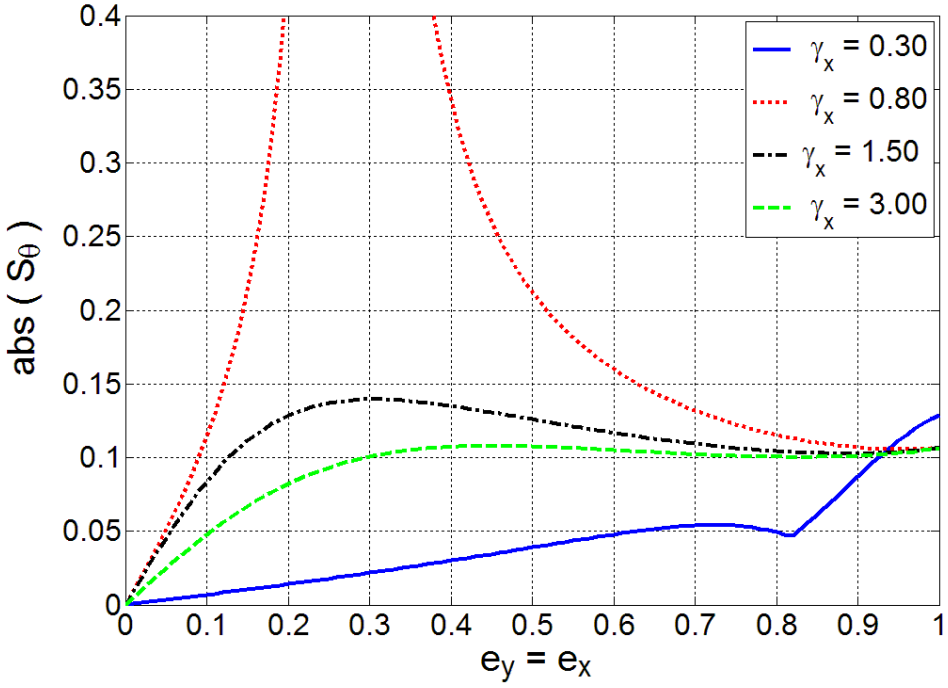

Figure 3.17 Variation of S_θ at the top of the flexural beam with eccentricity in both directions ($\gamma_\theta = 0.50$).

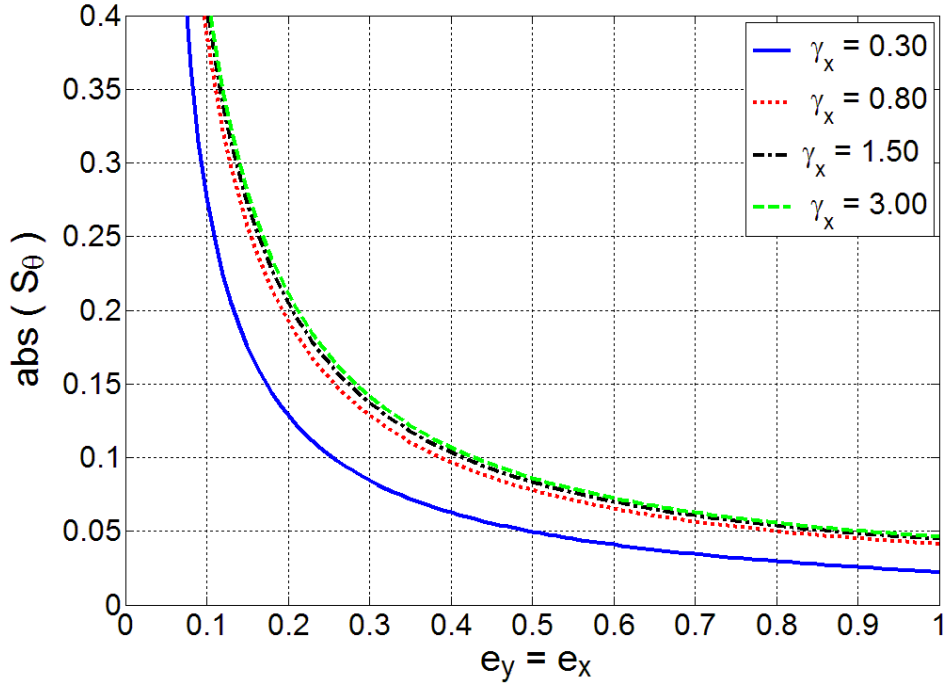

Figure 3.18 Variation of S_θ at the top of the flexural beam with eccentricity in both directions ($\gamma_\theta = 1.00$).

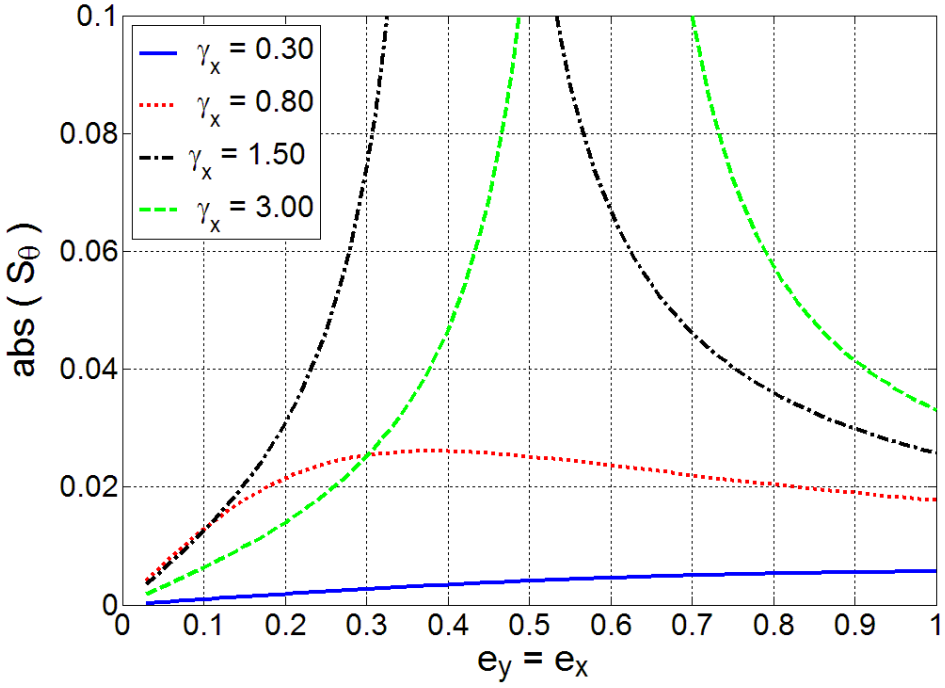

Figure 3.19 Variation of S_θ at the top of the flexural beam with eccentricity in both directions ($\gamma_\theta = 2.00$).

3.5 Shear Beam Model

The partial differential equation governing the vibration of a shear beam is hyperbolic and represents the wave propagation problem. In the most general case, just like flexural beam, the vibration of a shear beam with eccentricity is a set of three coupled partial differential equations. This system is shown in Equation (2.6). If the cross sectional area and eccentricity is assumed to be constant, the governing system of equation can be presented as:

$$\begin{cases} GA\left(\dfrac{\partial^2\delta_x}{\partial z^2}-e_y\dfrac{\partial^2\theta}{\partial z^2}\right)=m\dfrac{\partial^2\delta_x}{\partial t^2}-P_x\left(z,t\right) \\ GA\left(\dfrac{\partial^2\delta_y}{\partial z^2}+e_x\dfrac{\partial^2\theta}{\partial z^2}\right)=m\dfrac{\partial^2\delta_y}{\partial t^2}-P_y\left(z,t\right) \\ GA\left[e_x\dfrac{\partial^2\delta_y}{\partial z^2}-e_y\dfrac{\partial^2\delta_x}{\partial z^2}+\left(\lambda+e_x^2+e_y^2\right)\dfrac{\partial^2\theta}{\partial z^2}\right] \\ \qquad\qquad =I_o\dfrac{\partial^2\theta}{\partial t^2}-T\left(z,t\right) \end{cases} \tag{3.22}$$

Similar to the flexural beam, it is assumed that a constant eccentricity is applied in both directions and the load is a harmonic distributed load applied in x-direction. By changing this eccentricity the variation of response ratio at the tip of the beam has been presented in Figures (3.20) to (3.25). It should be mentioned that similar to flexural beam the following figures were prepared by solving the system of PDEs of Equation (3.22) in normalized space. The same numerical scheme as of previous section was used.

As it can be seen from these graphs, the shear beam model is showing the same behavior as the previous cases, thus the arguments and discussions are the same as before.

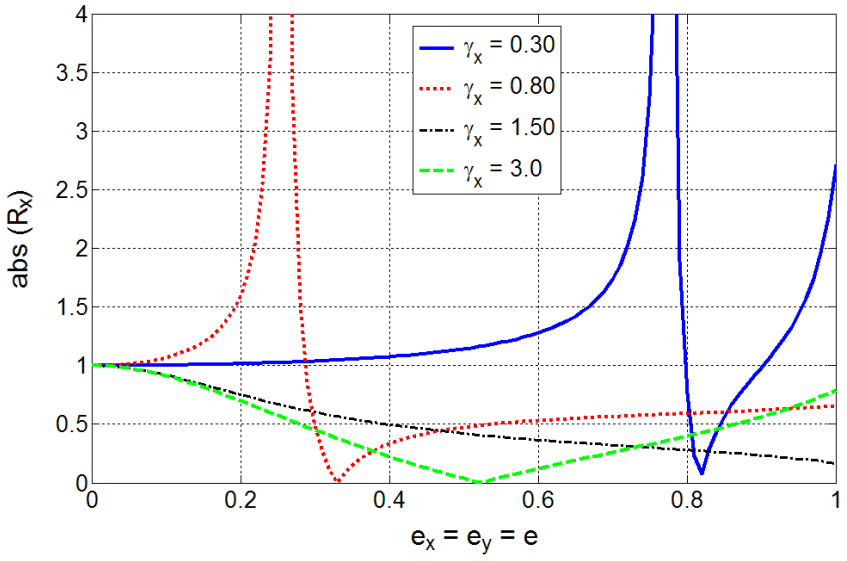

Figure 3.20 Variation of $\boldsymbol{R_x}$ at the top of a shear beam with eccentricity in both directions ($\gamma_\theta = 0.50$).

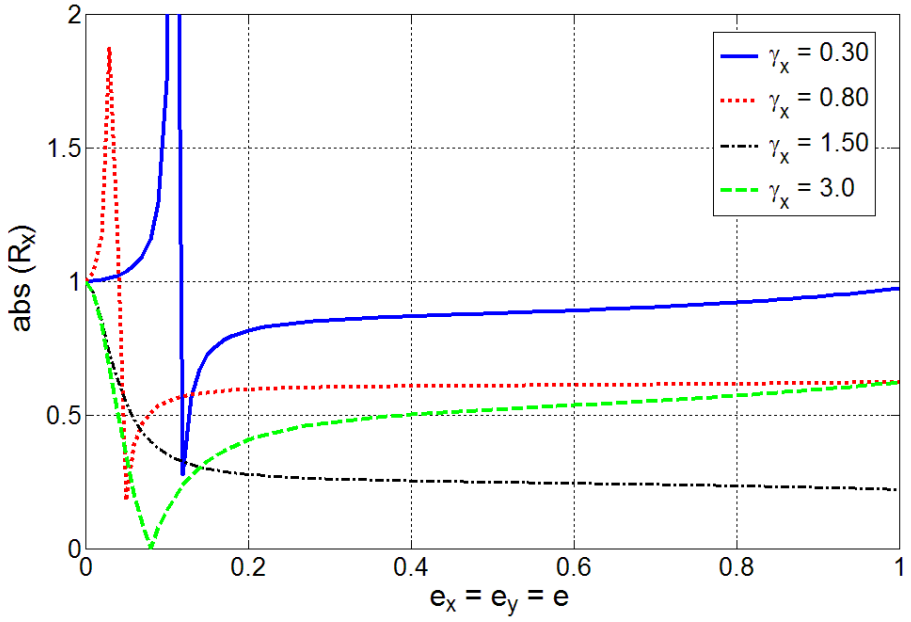

Figure 3.21 Variation of $\boldsymbol{R_x}$ at the top of a shear beam with eccentricity in both directions ($\gamma_\theta = 1.00$).

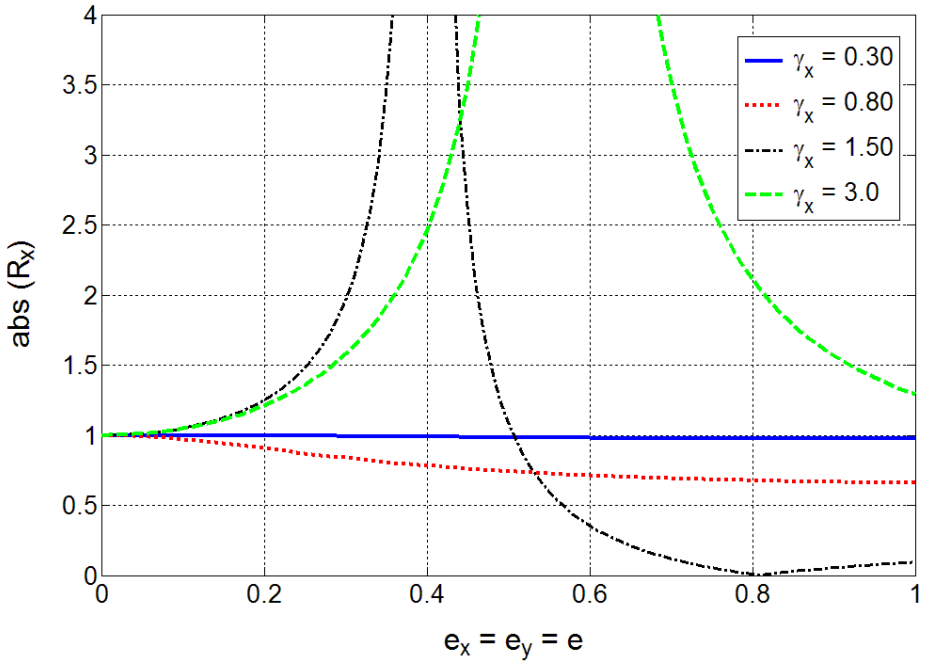

Figure 3.22 Variation of R_x at the top of a shear bean with eccentricity in both directions ($\gamma_\theta = 2.00$).

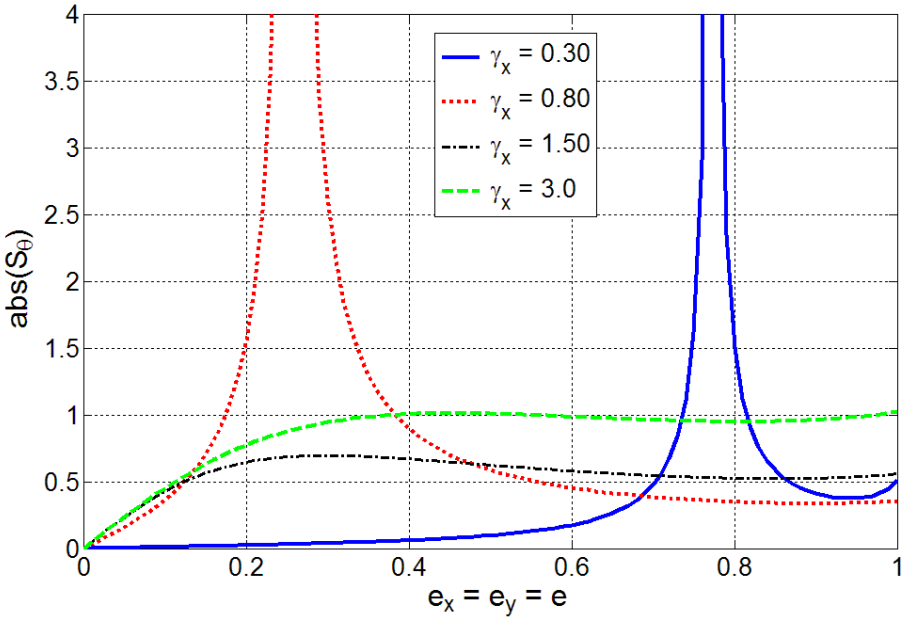

Figure 3.23 Variation of S_θ at the top of a shear beam with eccentricity in both directions ($\gamma_\theta = 0.50$).

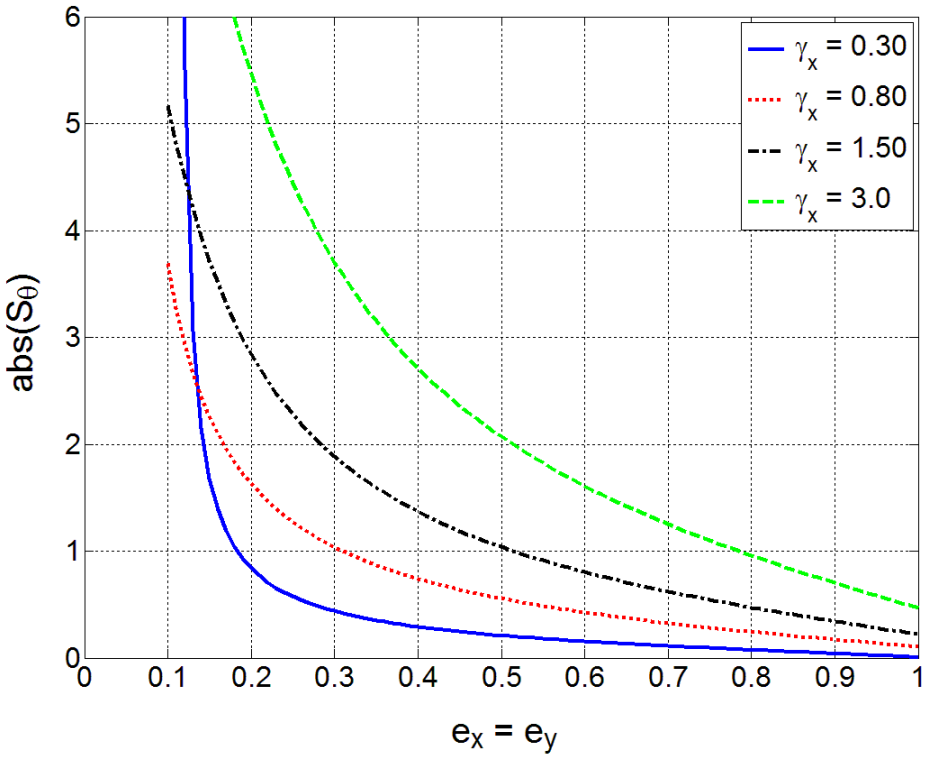

Figure 3.24 Variation of S_θ at the top of a shear beam with eccentricity in both directions ($\gamma_\theta = 1.00$).

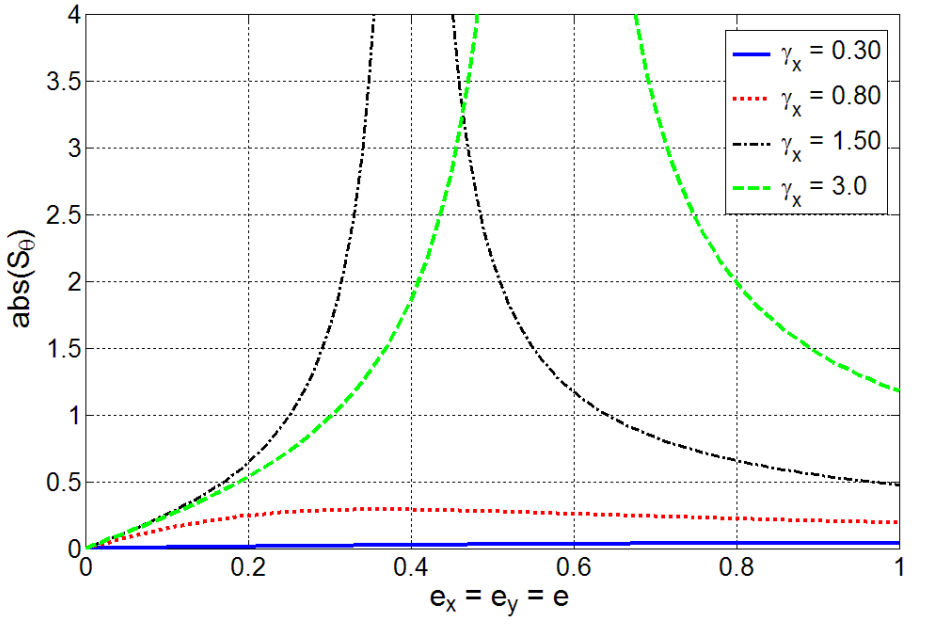

Figure 3.25 Variation of S_θ at the top of a shear bean with eccentricity in both directions ($\gamma_\theta = 2.00$).

CHAPTER 4

SEISMIC EFFECTIVENESS OF ECCENTRICITY IN MITIGATION OF TRANSLATIONAL RESPONSE

In Chapter 3 the focus was on the steady state response of eccentric structures. It was observed that eccentricity can indeed reduce the translational steady state response of different structural systems provided certain conditions are met. In this chapter the structural models are subjected to more realistic loads, and a comprehensive study is conducted to evaluate the seismic effectiveness of the proposed method with respect to reducing the translational displacement. To this end the structural models are exposed to a variety of earthquake records and the response ratios are statistically studied.

4.1 Statistical Analysis with Historical Earthquakes

The four structural models introduced in Chapter 2 are subjected to real earthquake records and the time history responses are evaluated carefully.

The earthquake records are acceleration time histories of a selection of major earthquakes that have happened all over the world in the past. One of the most important characteristics of an earthquake record is its frequency contents. This parameter is different from record to record and it could have a significant impact on the response. Therefore, it is tried to select the earthquake records in a way that they represent different site conditions and consequently cover a broad range of frequency contents. Based on the average shear wave velocity (Vs) to a depth of 30m, the United States Geological Survey (USGS) classifies the site conditions into four categories:

I. A: $Vs \geq 750$ m/s
II. B: 360 m/s $\leq Vs \leq 750$ m/s
III. C: 180 m/s $\leq Vs \leq 360$ m/s
IV. D: $Vs \leq 180$ m/s

This classification covers a broad range of site conditions from hard rock (category A) to soft soil (category D). Four records from each category is selected which altogether form an ensemble of sixteen earthquake records. The list of selected records is presented in Table 4.1. The records are picked from PEER Strong Motion Database. (http://peer.berkeley.edu/smcat/index.html).

Moreover the results of Chapter 3 show that the ratio of translational frequency to rotational frequency could play an important role in the amount of reduction in translational displacement. Thus, in order to take the effect of this factor into account, a new parameter denoted with Γ and called *frequency ratio* is defined as follows:

$$\Gamma = \frac{\omega_x^2}{\omega_\theta^2} \tag{4.1}$$

Since in most of structures the dominant mode of vibration is the translational mode, translational frequency would be smaller than torsional frequency. Thus for the most structures the frequency ratio will be smaller than one. Nevertheless, in order to cover a broad range of numbers for frequency ratio, eight numbers were selected as follows: 0.2, 0.5, 1.0, 2.0, 5.0, 10, 20 and 50.

To put the issue into perspective, the procedure of statistical analysis against historical earthquakes can be summarized as follows:

1. One structural model, out of four models introduced earlier, is selected.

2. An earthquake record is selected from Table 4.1.

3. A value for Γ is picked and while the translational stiffness is kept unchanged the rotational stiffness values are modified accordingly.

Table 4.1 List of Earthquake Records Selected for the Analyses

Site Condition	Record Number	Earthquake	Station	Record/Component	PGA (g)
A	1	Loma Prieta 1989/10/18	47379 Gilroy Array #1	LOMAP/G01090	0.473
	2	San Fernando 1971/02/09	127 Lake Hughes #9	SFERN/L09021	0.157
	3	Northridge 1994/01/17	24207 Pacoima Dam (upper left)	NORTHR/PUL104	1.585
	4	Kocaeli, Turkey 1999/08/17	Izmit	KOCAELI/IZT090	0.22
B	5	Kern County 1952/07/21	1095 Taft Lincoln School	KERN/TAF111	0.178
	6	Friuli, Italy 1976/09/15	8014 Forgaria Cornino	FRIULI/B-FOC270	0.212
	7	Kobe, Japan 1995/01/16	0 KJMA	KOBE/KJM000	0.821
	8	Loma Prieta 1989/10/18	58065 Saratoga - Aloha Ave	LOMAP/STG000	0.512
C	9	Central Calif 1960/01/20	1028 Hollister City Hall	CTRCALIF/B-HCH271	0.063
	10	Cape Mendocino 1992/04/25	89156 Petrolia	CAPEMEND/PET000	0.590
	11	Chi-Chi, Taiwan 1999/09/20	NST	CHICHI/NST-E	0.309
	12	Chi-Chi, Taiwan 1999/09/20	TAP042	CHICHI/TAP042-N	0.1
D	13	Imperial Valley 1979/10/15	5057 El Centro Array #3	IMPVALL/H-E03140	0.266
	14	Loma Prieta 1989/10/18	1002 APEEL 2 - Redwood City	LOMAP/A02043	0.274
	15	Kobe, Japan 1995/01/16	0 Takarazuka	KOBE/TAZ090	0.694
	16	Northridge 1994/01/17	90011 Montebello - Bluff Rd.	NORTHR/BLF206	0.179

4. Eccentricity is varied from 0 to 100% (with 10% increments) of allowable value and for each value a time history analysis is carried out. The maximum displacement in each time history analysis is found and the corresponding response ratio

is computed. It should be noted that the eccentricities are assumed to be constant over the height. Among the calculated response ratios in this step the smallest is selected.

5. Steps 1 to 4 are repeated for all the possible combinations of structural models, earthquake records, values of response ratios and eccentricities. The number of analyses would add up to 5632.

6. Finally, three major statistical parameters, namely: mean, median and standard deviation of response ratio are computed and different types of graphs are developed.

4.2 Seismic Effectiveness of Eccentricity as a Motion Control Strategy

The study presented in previous section is a comprehensive observation of the behavior of eccentric structures that could lead to a good understanding of the effectiveness of eccentricity as a motion control strategy. Since the number of analyses is high (1408 for each structural model), the results are expected to be solid and provide us with a decent estimation of the reductions that could be achieved under more realistic loadings.

The results of the analyses for different structural models are presented in Figure 4.1.

Figure 4.1 shows the average, mean and standard deviation of response ratios(R_x) for different structural models. An overall review of the graph indicates that the amount of reductions are significant. The average reductions achieved is from 20% to 30%. This proves the effectiveness of the proposed idea as a tool to mitigate the translational displacements. As it can be seen the average of reductions in a single story building, multistory building and flexural beam are about the same and around 32%. This is an indication of the fact that the performance of eccentric structure is independent of the

structural system as long these three models are concerned. However, with respect to the shear beam model, less amount of reduction is seen. The mean value of reduction in displacements is about 19% for this system.

Another interesting point about Figure 4.1 is the small difference between mean and median values. This fact along with the fact that the standard deviation values are rather small (less than 20%) indicates that the values of response ratios are clustered closely around mean and median. This point holds for all structural models.

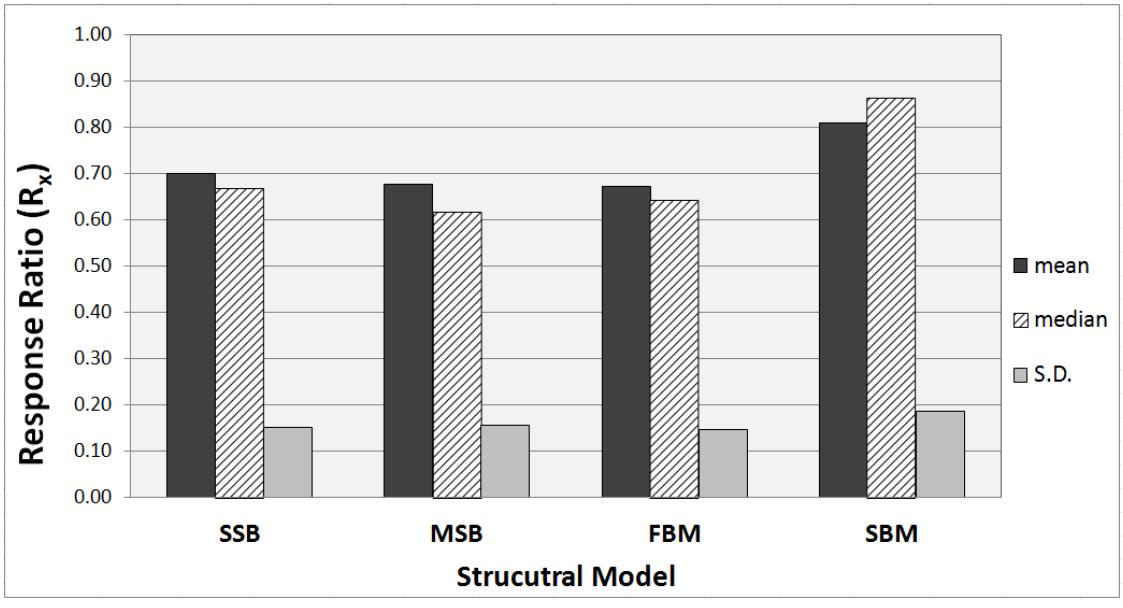

Figure 4.1 Mean, median and standard deviation of response of ratios.

4.3 Parametric Analysis of the Behavior of Eccentric Structures

4.3.1 Variation of Response Ratio with Frequency Ratio

The steady state analyses of Chapter 3 showed that the frequency ratio could have a significant impact on the level of reduction in translational displacement. In light of this

fact a key component of the statistical analysis of this chapter is studying the effect of frequency ratio on the variations of response ratio.

Figures 4.2 through 4.5 show the variations of mean, median and standard deviation of response ratio versus frequency ratio. The mean value graphs essentially represent the average of calculated minimum response ratios while the frequency ratio is set to a certain number. Medians and standard deviations are computed in a similar way.

Figures 4.2 to 4.5 indicate that the variation of mean value of response ratio with frequency ratio is more or less the same for all structural models. Nevertheless the behavior of shear beam model is slightly different. The trend of median and standard deviations are also the same in all figures. Therefore, it can be concluded that the behavior of eccentric structures are roughly the same regardless of their type and governing equations of motion.

As it can be seen the median is very close to the mean value and this does not depend on the frequency ratio. In other words median remains to be in a close vicinity of mean value for every frequency ratio. The values of the standard deviation shows to be about the same as the values shown in Figure 4.1. Actually this is an indication of the fact that the scattering of the response ratio values does not depend on the frequency ratio either and it remains to be the same as what is shown in Figure 4.1. This statement especially holds to be true when frequency ratio is more than one. As it was discussed earlier in structures with a frequency ration larger than one, the dominant mode of vibration is torsional rather translational.

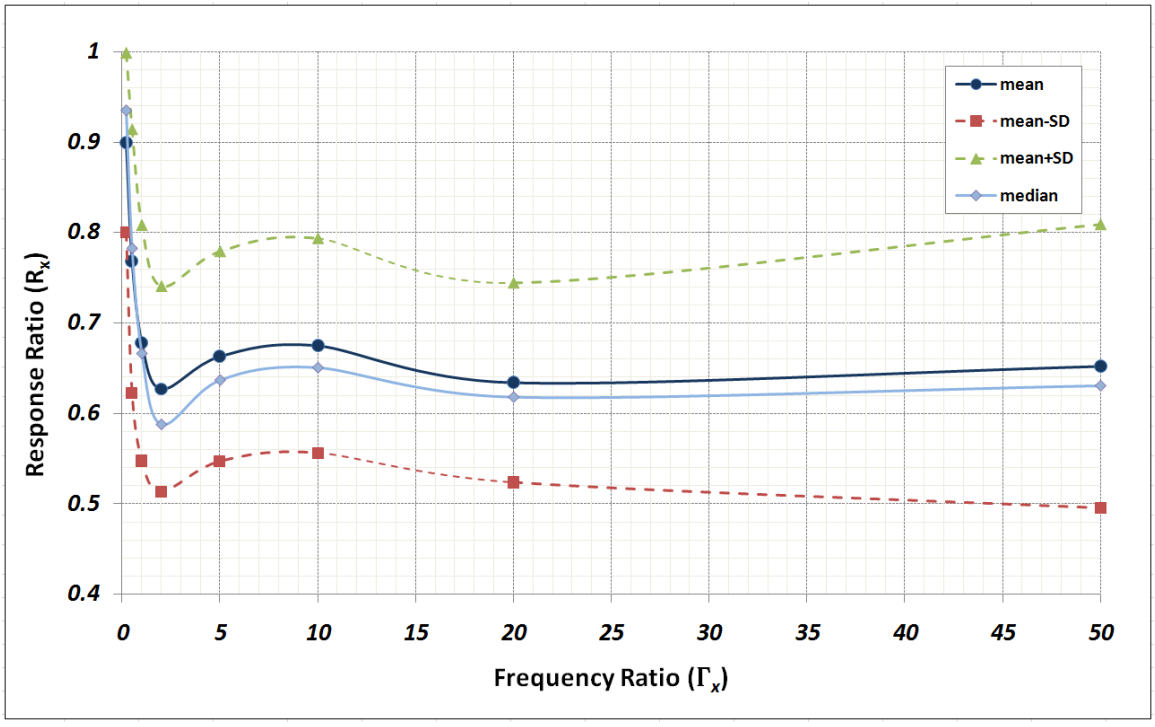

Figure 4.2 Variation of different statistical measures of response ratio with frequency ratio for the single story building model.

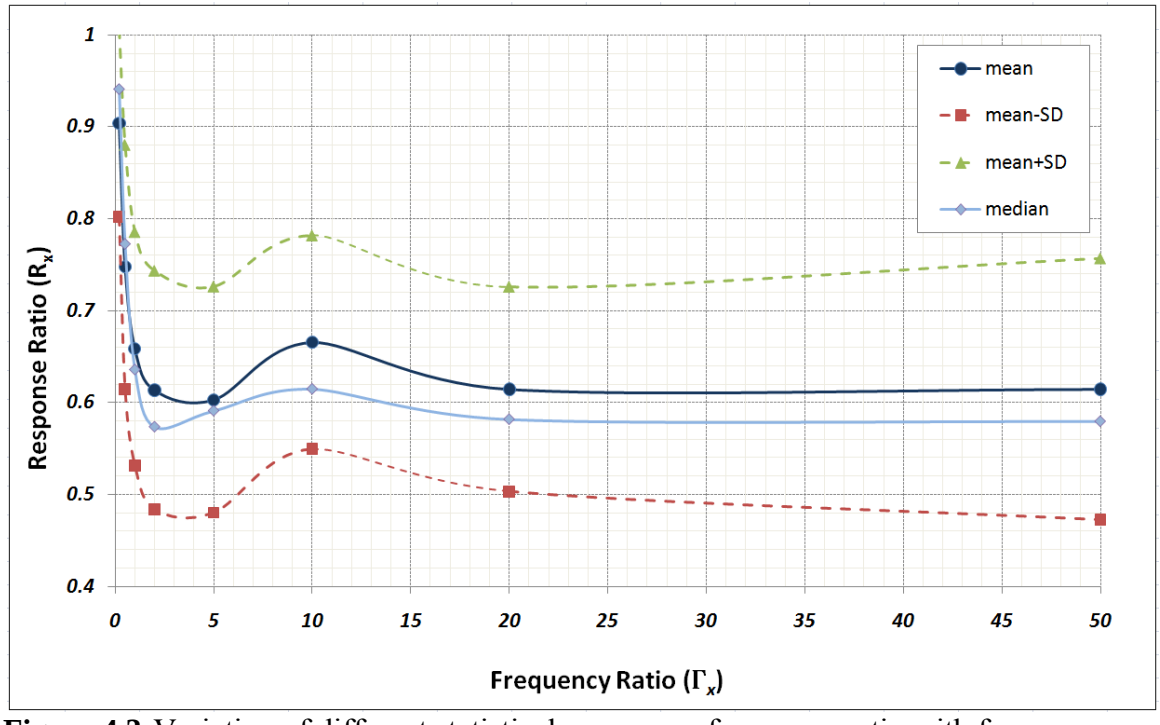

Figure 4.3 Variation of different statistical measures of response ratio with frequency ratio for the multi-story building model.

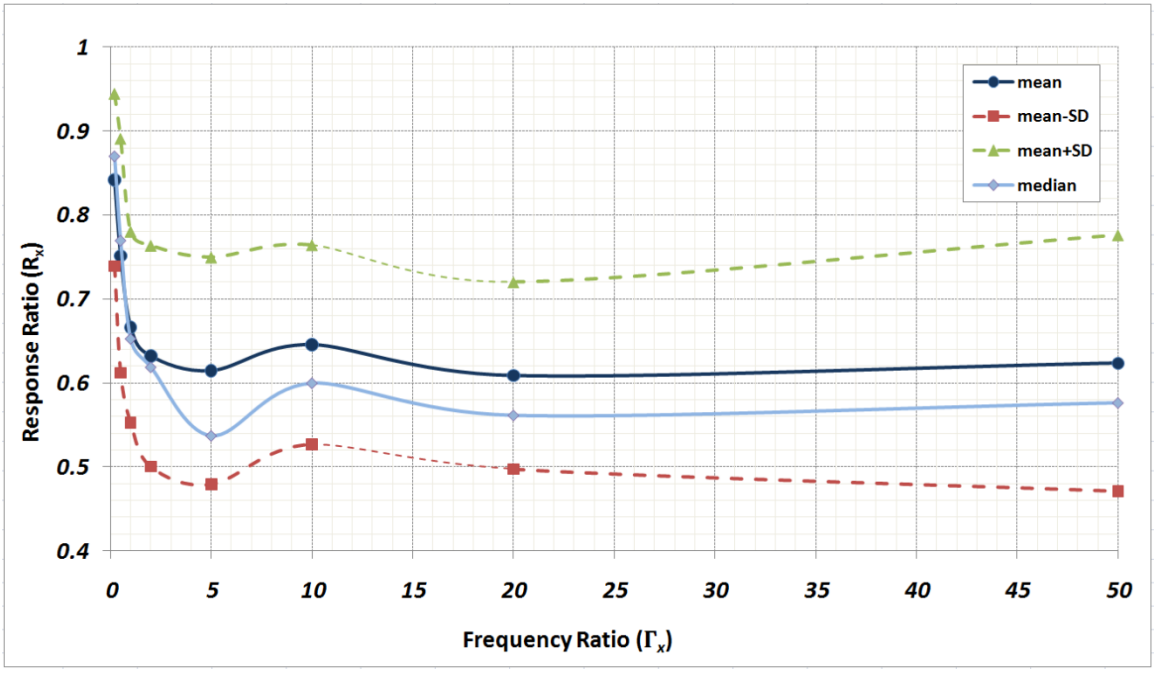

Figure 4.4 Variation of different statistical measures of response ratio with frequency ratio for the flexural beam model.

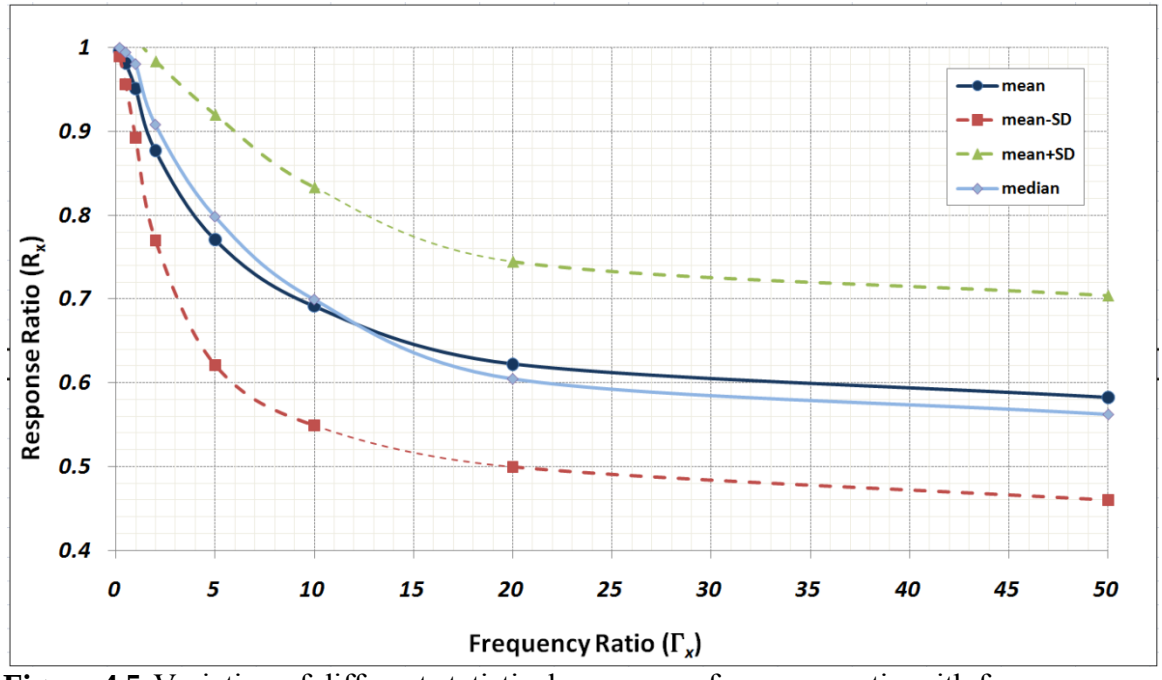

Figure 4.5 Variation of different statistical measures of response ratio with frequency ratio for the shear beam model.

Furthermore Figures 4.2 to 4.4 show that when frequency ratio is smaller than one the amount of reduction is significantly sensitive to the frequency ratio. This trend is different for shear beam. Because the response ratio remains sensitive to frequency ratio until frequency ratio reaches twenty. In any case, in all the structural models, when the frequency ratio is larger than a certain value the amount of reduction would become insensitive. This certain value would be called *sensitivity threshold*. It is easy to see that the amount of reduction is maximum when the frequency ratio is smaller than sensitivity threshold. Put differently, Figures 4.2 to 4.5 reveal that the minimum value of response ratio occurs when the frequency ratio is smaller than the value of sensitivity threshold. However, the response ratios corresponding to the frequency ratios larger than the threshold value are close to that minimum point. Therefore, it could be deducted that once the frequency ratio is larger than the sensitivity threshold the response ratio would not be sensitive to it and also its value is close to the minimum value that could be achieved. In addition to that it is an indication of the fact that for large frequency ratios, as far as the statistical analysis presented in this chapter is concerned, changing the rotational frequency did not affect the amount of reduction that could be achieved.

Finally for all the structural models the reductions are very small when the frequency ratio is small. In other words when the translational frequency is substantially smaller than rotational frequency the reductions in translational displacements are the least. On the other hand when torsional frequency is drastically smaller than translational frequency the reductions are closed to maximum. This phenomenon could be explained this way: the central idea behind using eccentricity in motion control is to reduce the translational vibration by engaging new modes of vibration including rotation. Therefore,

in a structure with a given translational stiffness more reduction is achieved if more rotation is allowed and this happens when the structure is designed rotationally more flexible. In such a structure the dominant mode of vibration would be torsional.

4.3.2 Variation of Response Ratio with Eccentricity

To gain more insight on the behavior of eccentric structures the variation of average of response ratios with eccentricity has been studied. In Figures 4.6 to 4.9 the variations of the average of response ratios vs. eccentricity is plotted for different structural systems. The main graph (solid line) is the average of mean response ratios of structures with different frequency ratios exposed to different seismic records. However, the variation of response ratio of each structure with different frequency ratio has been plotted separately also (dashed lines).More specifically, the solid curve is average of shown dashed lines. These dashed curves are the average of response ratios of structures with a specific frequency ratio exposed to the different earthquake records shown in Table 2.1.

Several observations can be made from Figures 4.6 to 4.9:

Initially, there is an eccentricity in all the four graphs for which the reduction is maximum. That point was called optimal eccentricity in Chapter 3. The maximum reduction is slightly larger than 15% for single story building, multi-story building and flexural beam and it is around 12% for shear beam. Therefore, the shown graphs prove that usually there is a point of optimal eccentricity and consequently the average reduction for that eccentricity is maximum.

Another interesting observation is the behavior of structures with different frequency ratios. It is easy to see that small frequency ratios would result in small

reductions and this statement is valid for all structural models. Moreover the maximum reductions are achieved for frequency ratios greater than the sensitivity thresholds introduced earlier in this chapter. This statement also holds to be true for all structural models and is in agreement with the results and conclusions gained in previous section. Similar to the previous section, the behavior of shear beam model is slightly different than that for other three models. Figure 4.9 shows that the amount of reduction is completely proportional to the frequency ratio. In other words the higher the frequency ratio the smaller the minimum response ratio. Figures 4.6 to 4.8 show that this is not the case. Because for these cases the minimum response ratio is achieved when Γ_x=2.0.

It should be mentioned that all of the above results support what can be seen in graphs 4.2 to 4.5.

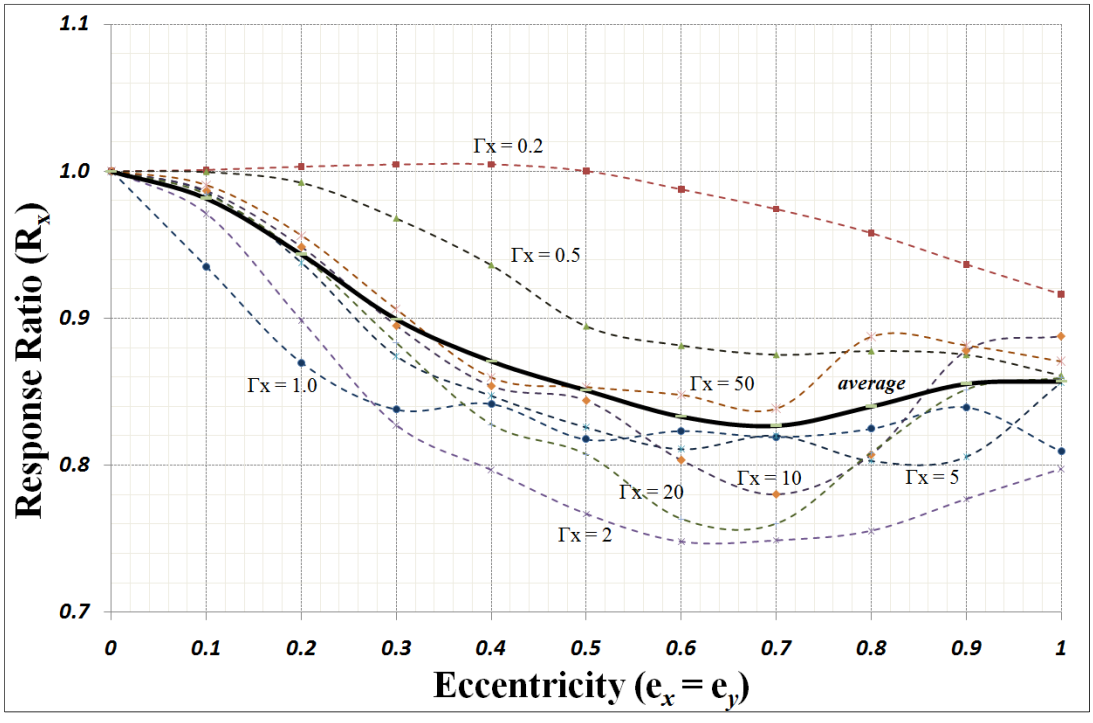

Figure 4.6 Variation of average response ratios with eccentricity for the single story building model.

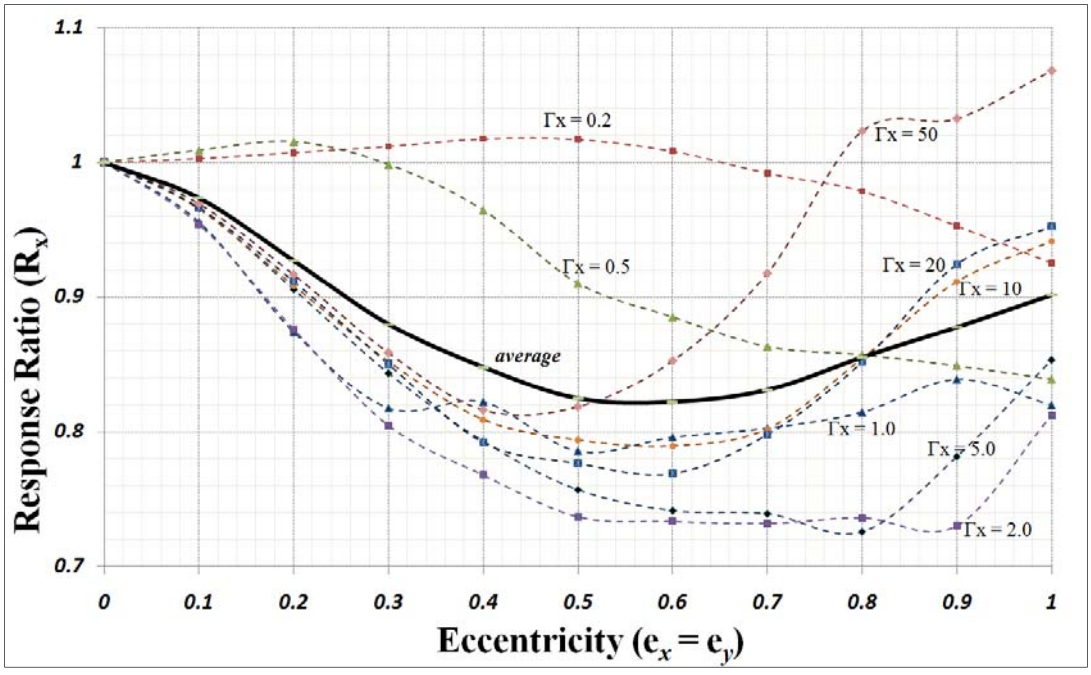

Figure 4.7 Variation of average response ratios with eccentricity for the multi story building model.

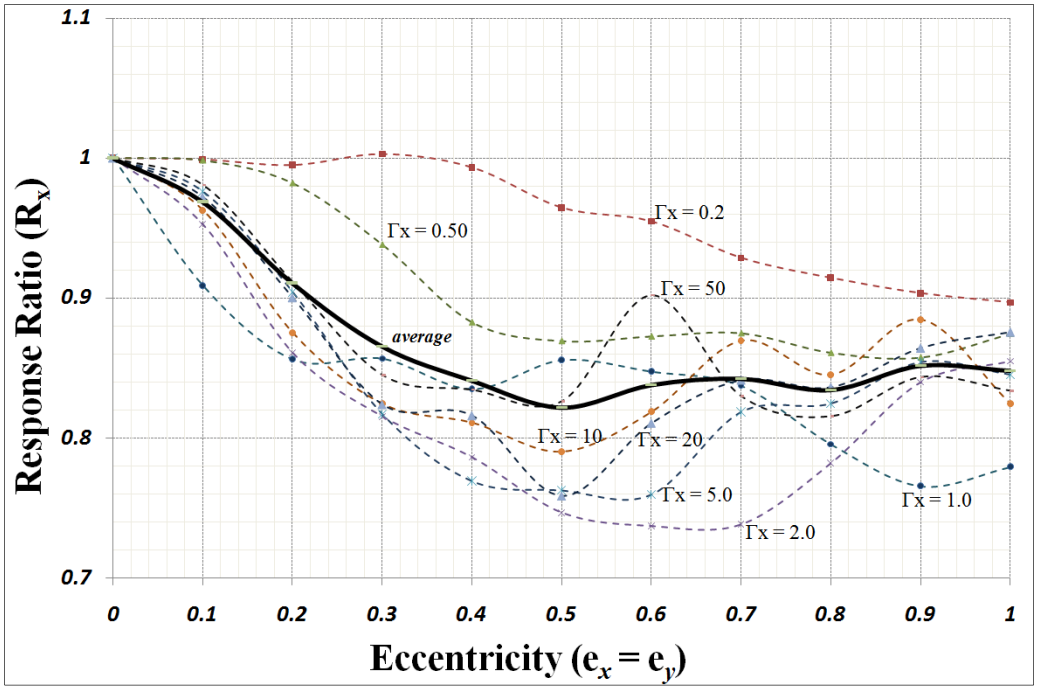

Figure 4.8 Variation of average response ratios with eccentricity for the flexural beam model.

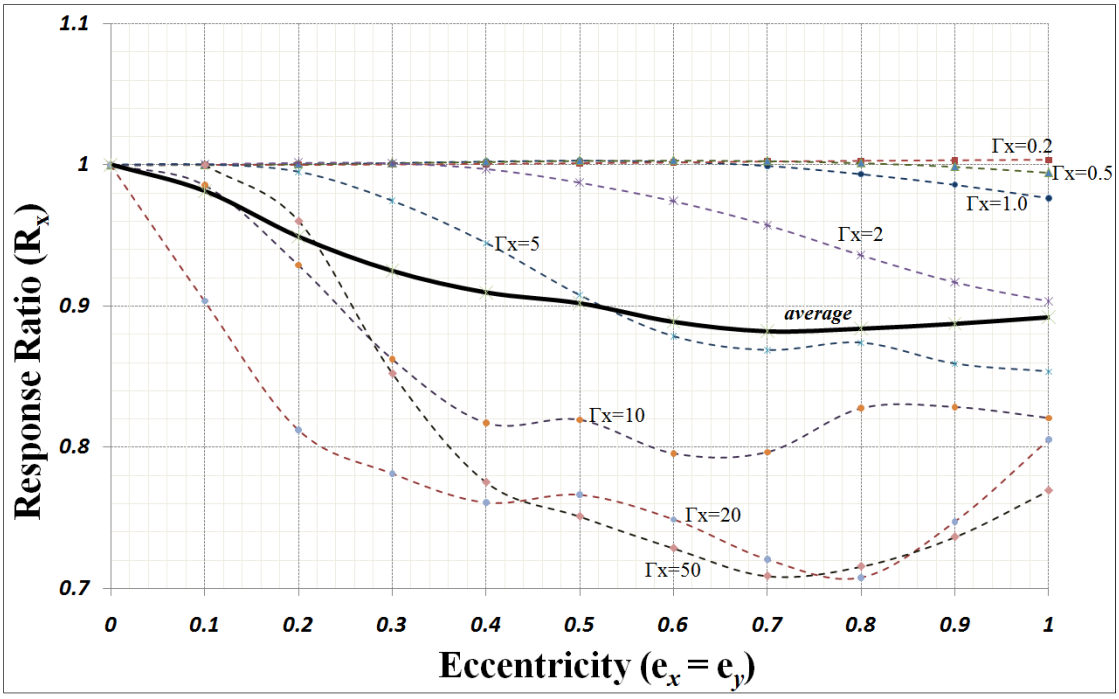

Figure 4.9 Variation of average response ratios with eccentricity for the shear beam model.

4.3.3 Time History Results

Finally, studying different time history responses could be very informative with regard to behavioral characteristics of eccentric structures. Time histories of displacement demonstrate how the behavior of a non-eccentric structure changes when eccentricity is applied. Since the number of analyses carried out are too many only four time histories of displacements are chosen to be plotted in Figures 4.10 to 4.13. These figures are a comparison between the behavior of non-eccentric and the corresponding eccentric structures. The presented time histories represent a variety of site conditions and frequency ratios. All the eccentricities selected for the analyses are the optimal eccentricity for that particular earthquake record.

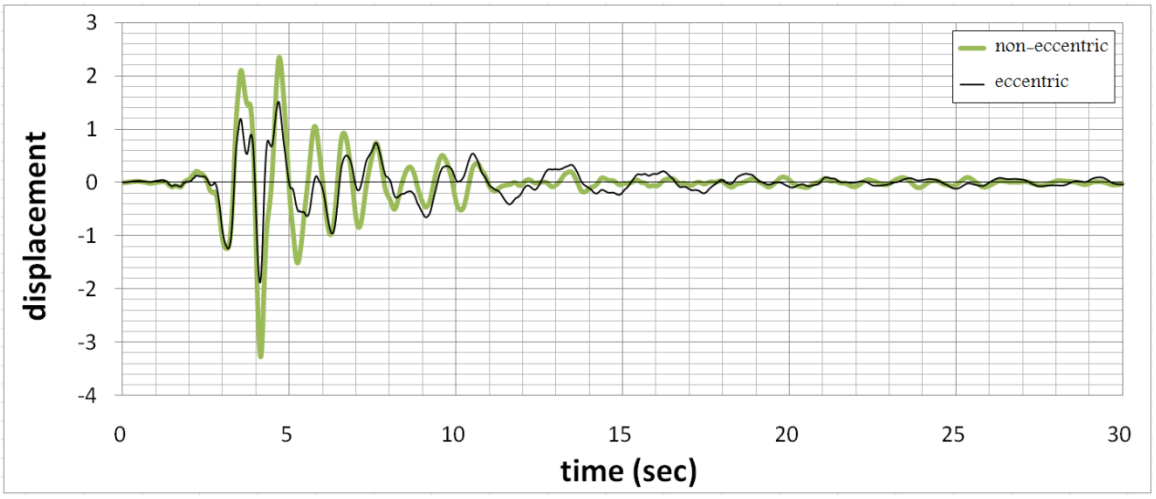

Figure 4.10 Time history responses of a non-eccentric and corresponding eccentric single story building to San Fernando record (#2, Table 4.1). $\Gamma_x = 5.0$ and eccentricity is 60% of the allowable eccentricity.

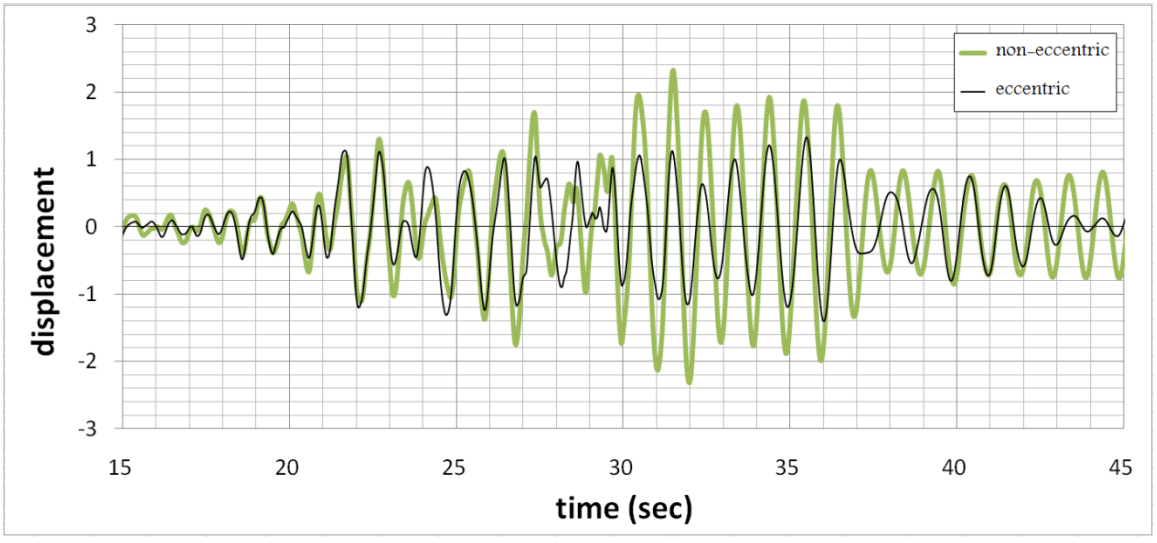

Figure 4.11 Time history responses of a non-eccentric and corresponding eccentric multi story building to Chi-Chi Taiwan record (#11, Table 4.1). $\Gamma_x = 1.0$ and eccentricity is 70% of the allowable eccentricity.

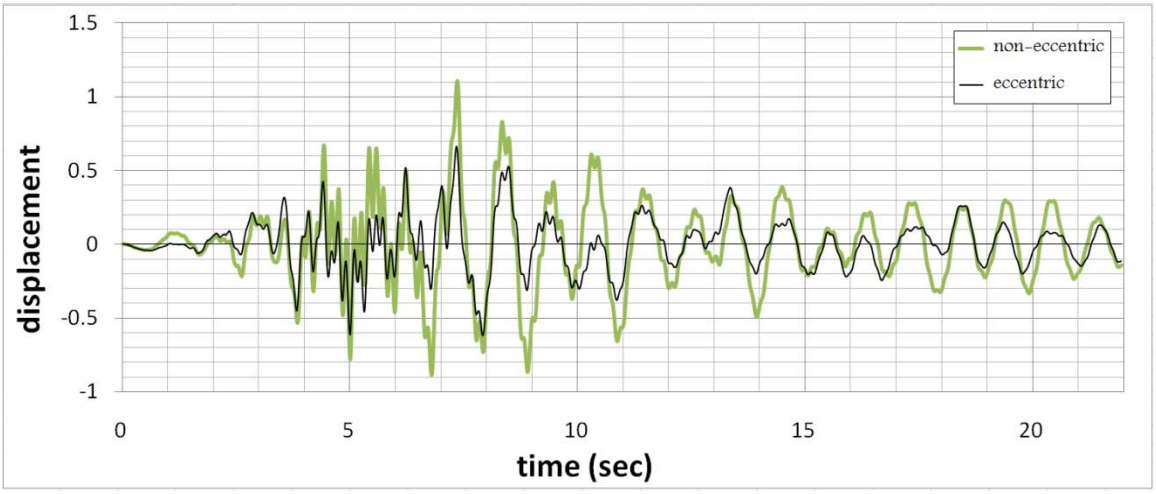

Figure 4.12 Time history responses of a non-eccentric and corresponding eccentric flexural beam to Kern County record (#5, Table 4.1). $\Gamma_x = 20.0$ and eccentricity is 30% of the allowable eccentricity.

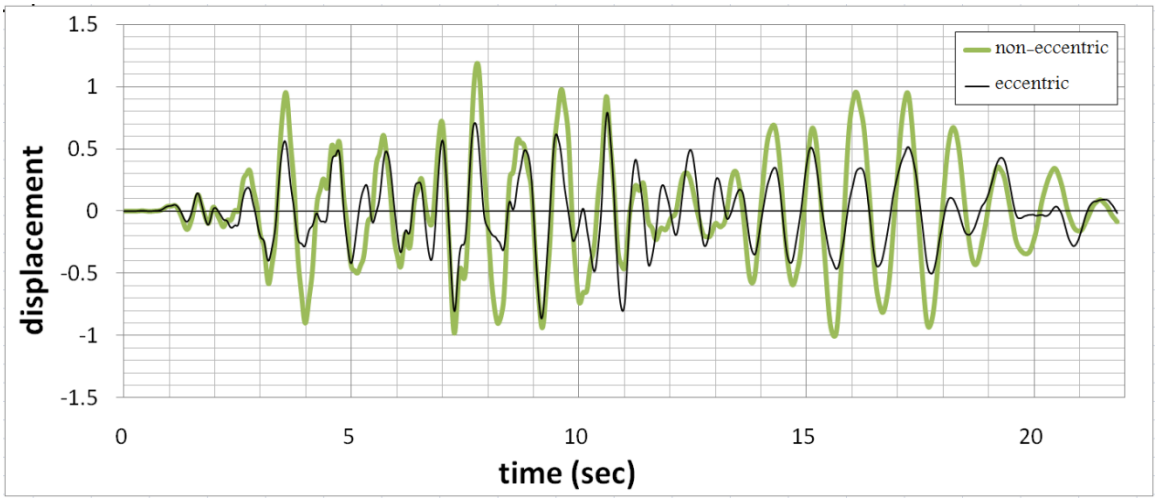

Figure 4.13 Time history responses of a non-eccentric and corresponding eccentric shear beam to Northridge record (#16, Table 4.1). $\Gamma_x = 50.0$ and eccentricity is 90% of the allowable eccentricity.

By studying Figures 4.10 through 4.13 several interesting observations can be made as follows:

To begin with, the frequencies of eccentric and non-eccentric structures are different. The larger the eccentricity the greater the difference between the two frequencies. This could be explained this way: by introducing the eccentricity the

stiffness matrix of the non-eccentric structures changes, while the mass matrix remains to be the same. Therefore, the eigenvalues are going to be different. In other words, by applying eccentricity the dynamic properties of structure is changed.

Another interesting point that can be seen in the above figures is the fact that the time for which the maximum displacement occurs is not necessarily the same for the eccentric and corresponding non-eccentric structure. As an example in Figure 4.13 the non-eccentric structure reaches its maximum after about 7.8 seconds, while this time for eccentric structure is 10.7 seconds.

4.4 A Final Point

It is important to note that the values shown in Figure 4.1 are the mean values of response ratios of structures with a wide variation in dynamic properties. To be more specific, all of the dynamic properties included in statistical analysis were not adjusted to provide the conditions for which the most reduction is achieved. Therefore, once the eccentricity as well as the dynamic properties of the structure are designed for a particular loading conditions i.e. earthquake record characteristics, the amount of reductions are expected to be more than the average values shown in Figure 4.1. In a similar format Figure 4.14 represents the minimum response ratios that were achieved for each structural systems.

This figure is plotted based on the minimum response ratios found throughout all the time history analyses performed for each structural model. The reductions shown in this figure are about 55%. The values in Figure 4.14 could be interpreted as the reductions that potentially could be achieved provided the dynamic properties of the structures along

with eccentricities are designed properly for a certain loading condition. It is easy to see that all the four structural models seem to have about the same minimum response ratio.

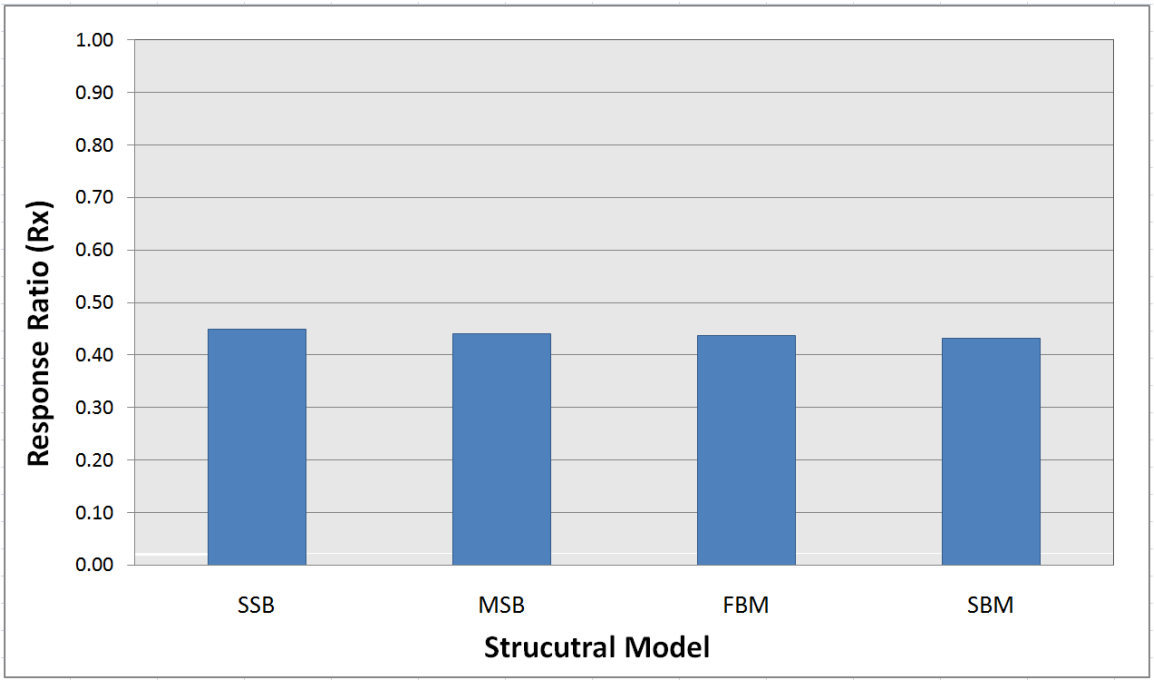

Figure 4.14 The minimum values of response ratio for different structural systems.

CHAPTER 5

OPTIMAL DESIGN OF ECCENTRICITY FOR SEISMIC APPLICATIONS

Translational displacements are one of the indexes of structural serviceability. Designers are always looking for ways to minimize it. In light of this fact the main objective of this chapter is to develop a systematic approach to maximize the reductions in translational vibration. The results of Chapters 3 and 4 show that eccentricity can drastically impact the dynamic response. In addition to eccentricity, frequency ratio turned out to play a significant role in the amount of reduction as well. The problem that is going to be solved herein can be expressed in this way: A structure with specific translational frequency is given. If the structure is subjected to base excitation, what is the eccentricity and frequency ratio for which the maximum reduction in translational displacements can be achieved? This eccentricity is called *optimal eccentricity*.

In this chapter the optimal design problem is formulated first. The design parameters would include eccentricity and frequency ratio. The theories of random vibration and optimal control are incorporated into the problem formulation to accommodate various challenges. These challenges will be discussed in more detail in the sections that follow. After the formulation of the optimization problem two structural models are studied through examples. Similar to the previous chapters the simplest model which is a single story building would be discussed first. Again since the numbers of state variables are few it is easier to analyze the behavior of this structural model.

Next model to study is the multi-story building. The optimization problem for this case is studied with two different assumptions. First it is assumed that eccentricity is constant over the height. In this case the numbers of state variables are only two:

constant eccentricity and frequency ratio. Second assumption is that the eccentricity could be variable over the height. In other words in this case the optimal distribution of eccentricity over the height is sought. The number of state variables in this case could be very large and comparing to the constant eccentricity case it is a more difficult problem to solve.

This chapter continues with a case study. The main objective of the case study is to compare the performance of the proposed strategy with that of an existing passive control such as tuned mass dampers (TMD). This model would be among those in the literature for which the effectiveness of TMD has already been tested. Based on the approach developed in this chapter optimal eccentricity and frequency ratio are applied to the same model and the reductions are compared with those of TMDs.

5.1 Formulation of the Optimization Problem

5.1.1 Governing Equations of Motion

In time domain the equations of motion of a structure with 3n degrees of freedom that is subjected to base excitation can be described as:

$$\boldsymbol{M}\ddot{\boldsymbol{\delta}}(t)+\boldsymbol{C}\dot{\boldsymbol{\delta}}(t)+\boldsymbol{K}\boldsymbol{\delta}(t)=\boldsymbol{f}_g(t) \tag{5.1}$$

where $\boldsymbol{\delta}(t)$ is the 3n×1 displacement vector and **M**, **C** and **K** are mass, damping and stiffness matrixes respectively. $\boldsymbol{f}_g(t)$ is the ground motion function and is described as :

$$\boldsymbol{f}_g(t)=-\boldsymbol{M}\boldsymbol{r}\,\ddot{\delta}_g(t) \tag{5.2}$$

In which $\ddot{\delta}_g(t)$ is the ground acceleration and *r* is a 3*n*×1 location vector and for the purpose of this thesis, since the earthquake is applied only in *x*-direction, it is expressed as :

$$\boldsymbol{r} = [100\ 100\ \ 100 \ldots 100 \ldots 100]^T \tag{5.3}$$

Now by taking a Fourier Transform to both sides of Equation (5.1) the analysis could be transformed from time domain into frequency domain and the result can be shown as :

$$\left(-\omega^2 \boldsymbol{M} + i\omega \boldsymbol{C} + \boldsymbol{K}\right) \boldsymbol{D}(\omega) = \boldsymbol{F}_g(\omega) \tag{5.4}$$

where $i = \sqrt{-1}$ and $\boldsymbol{D}(\omega)$ is the Fourier transforms of $\boldsymbol{\delta}(t)$. $\boldsymbol{F}_g(\omega)$ is the Fourier transform of ground motion function and is expressed as:

$$\boldsymbol{F}_g(\omega) = -\boldsymbol{M}\boldsymbol{r}D_g(\omega) \tag{5.5}$$

in which $D_g(\omega)$ is the Fourier transform of ground acceleration function.

Assuming:

$$\boldsymbol{Z}(\omega) = -\omega^2 \boldsymbol{M} + i\omega \boldsymbol{C} + \boldsymbol{K} \tag{5.6}$$

then $\boldsymbol{D}(\omega)$ can be readily found from Equation (5.4) :

$$\boldsymbol{D}(\omega) = \boldsymbol{Z}^{-1}(\omega)\boldsymbol{F}_g(\omega) \tag{5.7}$$

Usually $\boldsymbol{Z}^{-1}(\omega)$ is shown as $\boldsymbol{H}(\omega)$ and is called frequency response matrix or transfer function. Thus the equation of motion in frequency domain can be expressed in its simplest form as:

$$\boldsymbol{D}(\omega) = \boldsymbol{H}(\omega)\boldsymbol{F}_{\boldsymbol{g}}(\omega) \tag{5.8}$$

Basically $\boldsymbol{H}(\omega)$ is a function that bears the dynamic properties of the structure and is a mathematical representation of the relation between loading and response of the structure. For a 3n degree of freedom model this function is a $3n \times 3n$ matrix.

If ground motion function $\boldsymbol{f}_{\boldsymbol{g}}(t)$ is stochastic then the response $\boldsymbol{\delta}(t)$ would be stochastic as well. In this case the relation between the Power Spectral Density Function (PSDF) of response and excitation is described as follows:

$$\boldsymbol{S}_{\delta} = \boldsymbol{H}(\omega)\boldsymbol{S}_{f}\ \boldsymbol{H}^{T}(\omega) \tag{5.9}$$

in which :

$$\boldsymbol{S}_{f}\ = (-\boldsymbol{Mr})S_{g}\ (-\boldsymbol{Mr})^{T} \tag{5.10}$$

$\boldsymbol{S}_{\delta}$ and $\boldsymbol{S}_{f}$ are respectively the PSDF matrixes of response and ground motion. Both of these matrixes are $3n \times 3n$. Superscript T denotes the transpose or complex conjugate gradient of a matrix or a vector . S_g is the PSDF of the earthquake excitation.

Finally by substituting Equation (5.10) in (5.9) the PSDF of response can be re-written as :

$$\boldsymbol{S}_{\delta} = \boldsymbol{H}(\omega)(\boldsymbol{Mr})\ S_{g}\ (\boldsymbol{Mr})^{T}\ \boldsymbol{H}^{T}(\omega) \tag{5.11}$$

If one is interested in an *r*-component response vector $\boldsymbol{u}(t)$ as given in the time and frequency domains respectively by:

$$\boldsymbol{u}(t) = \boldsymbol{B} \,.\, \boldsymbol{\delta}(t) \tag{5.12}$$

$$\boldsymbol{U}(\omega) = \boldsymbol{B} \,.\, \boldsymbol{D}(\omega) \tag{5.13}$$

Where B is a $r \times 3n$ coefficient matrix, the $r \times r$ spectral density matrix for vector $\boldsymbol{u}(t)$ is then given by:

$$\boldsymbol{S}_u = \boldsymbol{B}\, \boldsymbol{S}_\delta\, \boldsymbol{B}^T \tag{5.14}$$

Equations (5.12) to (5.14) are useful when only the displacements and/or rotation of top floor are selected for study.

5.1.2 Power Spectral Density of Ground Motion

In real world prediction of a future earthquake is impossible. Thus a serious challenge in optimal design for seismic applications is the uncertainties of ground motion.

There are different ways to tackle this challenge. An option is to select an ensemble of earthquakes that represent the site condition of structure. Then similar to the previous chapter displacement vs. eccentricity graphs are developed for the range of allowable eccentricities. If constraints are imposed on rotations then rotational displacement vs. eccentricity graphs should be developed too. Using these two types of graphs the feasible amount of eccentricity for which the probability of maximum reduction is high could be obtained.

This approach is a robust method. However, the high computation cost is one of the disadvantages of this method. Moreover, it is very difficult to manage the huge amount of information obtained from numerous time history analyses. Because in order to find the optimum eccentricity a series of time histories analyses with all the possible eccentricities should be performed and then by comparing the results the optimum value should be found. Doing the time history analysis for several values of eccentricity and different records is computationally expensive and hard to deal with. Therefore, this method is considered to be costly.

Another method to approach this problem is using the concepts of optimal control theory and random vibrations. In this approach the ground motion is modeled as a stationary stochastic process. For this purpose the Power Spectral Density Function proposed by Kanai (Kanai 1957, 1961) and Tajimi (Tajimi 1960) is used to model the ground motion. This PSDF is expressed as:

$$S_g(\omega) = \frac{\omega_g^4 + 4\xi_g^2\omega_g^2\omega^2}{\left(\omega_g^2 - \omega^2\right)^2 + 4\xi_g^2\omega_g^2\omega^2} \tag{5.15}$$

where ω_g and ξ_g are characteristics ground frequency and damping ratio, respectively. By proper selection of these two parameters the above equation can be used to generate different spectral density shapes. It is shown in Figure 5.1 that Equation (5.15) captures well the frequency content of historical seismic events such as El Centro ($\omega_g = 12$ and $\xi_g = 0.6$) and Kobe ($\omega_g = 12$ and $\xi_g = 0.3$) (Hoang 2008). El Centro is the N-S component recorded at the Imperial Valley in El Centro during the Imperial Valley, California earthquake of May 18, 1940 and Kobe is the N-S component recorded at the

Kobe Japanese Meteorological Agency (JMA) station during the Hyogo-ken Nabu earthquake of January 17, 1995.

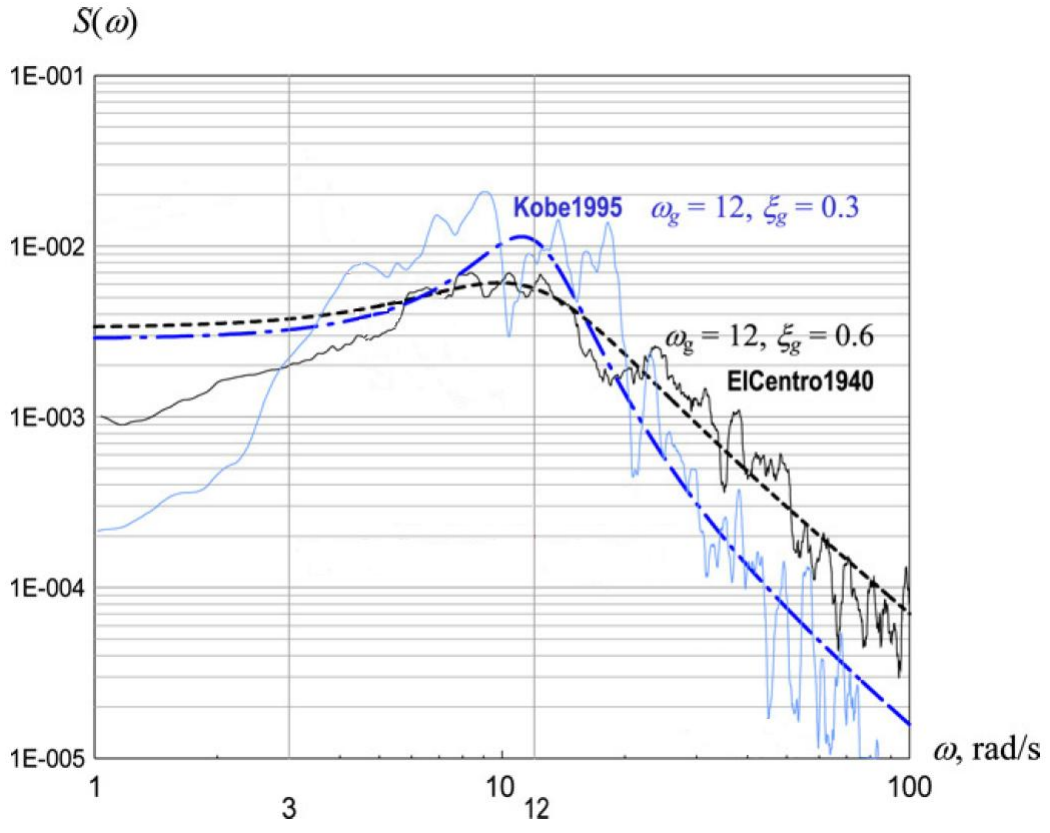

Figure 5.1 Comparison of Kanai–Tajimi PSDF with the actual ones for El Centro and Kobe records (Hoang 2008).

This approach for modeling of ground motion has been widely used in literature and it has proven to be successful in optimal design of other passive control systems such as tuned mass dampers (TMD) (Hoang et al. 2008, Chen et al. 2001, Lee et al. 2006 and Li et al. 2004).

5.1.3 Performance Index

An important part of an optimization problem is selecting the appropriate objective function. In optimal control theory this objective function is referred to as *performance index*. A performance index is a quantitative measure of the performance of a system and is chosen so the emphasis is given to the important system specification (Dorf and Bishop, 2005). A system is considered an optimum control system when the system parameters are adjusted so the index reaches an extremum, commonly a minimum value (Dorf and Bishop 2005).The selection of a particular performance index is determined by the objectives of the optimization problem. The performance index may be defined in different ways such as the integral of a function of the error variable that must be minimized (Ogata 1990).

Since the analyses are performed in frequency domain and the ground motion is modeled as a stochastic process, a convenient performance index (i.e. objective function) to use is the integral of the PSDF of the structural response with respect to frequency (Hoang 2008, Lee et. al 2006, Hoang 2005 and Chen 2001). This integral is basically the mean square value of the structural response. For the purpose of this thesis we are only interested in translational vibration of the top floor, therefore, the performance function is defined as:

$$J_{top} = E(\delta_{top}^2) = \boldsymbol{l}^T \left(\int_{-\infty}^{+\infty} \boldsymbol{S}_\delta d\omega \right) \boldsymbol{l} \tag{5.16}$$

in which E(.) represents the expected value or mean and $\boldsymbol{l}$ is a $3n\times1$ vector and is defined as:

$$\boldsymbol{l} = [000....100]^T \tag{5.17}$$

5.1.4 Constraints

There are two important types of constraints in the problem of finding the optimal eccentricity. One type of these constraints represents the limitations on the rotation and the other type restrains the maximum value that eccentricity can have. In this section these two types of constraints are explained in more detail.

5.1.4.1 Serviceability Constraints on Rotation. On one hand preliminary results from previous chapters show that eccentricity can actually reduce the translational vibration and on the other hand applying eccentricity is always accompanied by activation of rotational degree of freedom. Rotations are sometimes undesirable and serviceability limitations imposed by the codes would not allow the rotation to exceed a certain amount. If the allowable rotations are exceeded then the design is considered to be infeasible.

For building structures, the ASCE7-05 code imposes some limitations on story drift (ASCE7-05). These allowable story drifts are summarized in Table 12.12-1 of ASCE7-05. According to this table the allowable story drifts are in the range of $0.01h$ to $0.025h$, where h is the story height. In addition to that under section 12.12.1 of the same code it is explicitly mentioned that for the structures with significant torsional deflections the maximum drift shall include torsional effects as well.

As for nonbuilding structures the same code under section 15.4.5 states that the above mentioned drift limitations need not to be applied, if a rational analysis indicates they can be exceeded without adversely affecting structural stability or attached or interconnected components and elements.

The structural models used for this thesis are mathematical models and they are meant to provide a simulation of the behavior of a broad range of building and nonbuilding structures. Therefore, it is thought that considering an allowable drift of $0.02h$ is within a reasonable range. However, selecting this value does not hurt the generality of the proposed approach and the allowable drift could be different for different problems.

Since the torsional effect is supposed to be included in the displacement, drift limitation should be imposed at a point on the plan for which torsion is having the most adverse effect. These points are usually located at the corners of the floor. Thus, the rotational constraints are expressed as follows:

$$\delta^*_{x_{top}} = \delta_{x_{top}} - \left(\frac{a}{2}\right)\theta_{top} \leq 0.02h \tag{5.18}$$

$$\delta^*_{y_{top}} = \delta_{y_{top}} + \left(\frac{b}{2}\right)\theta_{top} \leq 0.02h \tag{5.19}$$

In which $\delta^*_{x_{top}}$ and $\delta^*_{y_{top}}$ are the displacements at the corners of top floor, $\delta_{x_{top}}$, $\delta_{y_{top}}$ and θ_{top} are the displacements and rotation of the center of mass, a and b are the dimensions of the top floor in x and y direction and finally h is the height of the structure.

Since the optimization problem as well as the governing equations are solved in the frequency domain and in addition to that PSDF of response are convenient to evaluate, the constraints of Equations (5.18) and (5.19) are incorporated in the optimization problem as follows:

$$\sqrt{J_{x_{top}}} - (\frac{a}{2})\sqrt{J_{\theta_{top}}} \leq 0.02h \tag{5.20}$$

$$\sqrt{J_{y_{top}}} + (\frac{b}{2})\sqrt{J_{\theta_{top}}} \leq 0.02h \tag{5.21}$$

In the above equations:

$$J_{y_{top}} = E(\delta^2_{y_{top}}),\ J_{x_{top}} = E(\delta^2_{x_{top}}) \text{ and } J_{\theta_{top}} = E(\delta^2_{\theta_{top}}) \tag{5.22}$$

As it was mentioned earlier E(.) represents the expected value of a variable. The mean square values in Equations (5.20) and (5.21) are calculated in a similar manner to that of Equation (5.16).

5.1.4.2 Physical Constraints on Eccentricity. There are physical limitation on the amount of eccentricity. These limitations are incorporated in the optimization problem as constraints. These constraints are mathematically described as:

$$\left|e_{x_i}\right| \leq e_{x_{all}} \tag{5.23}$$

$$\left|e_{y_i}\right| \leq e_{y_{all}} \tag{5.24}$$

In which e_{x_i} and e_{y_i} are the eccentricities in *x* and *y* direction in the i^{th} floor and $e_{x_{all}}$ and $e_{y_{all}}$ are the allowable eccentricities in *x*- and *y*-direction respectively. Usually in buildings it is physically impossible for eccentricity to exceed half of the length of the floor. Therefore, for the purpose of this research this value is selected as the allowable eccentricity.

5.1.5 Final Formulation of the Mathematical Programming

Once the governing equations, objective functions and constraints are determined the final formulation of the mathematical programming can be summarized as follows:

$$\textit{minimize}\ \ J\left(\boldsymbol{e}\ ,\ \Gamma_x\right)=\boldsymbol{l}^T\left(\int_{-\infty}^{+\infty}\boldsymbol{S}_\delta d\omega\right)\boldsymbol{l} \tag{5.25}$$

$$\textit{subject to}:$$

$$g_x\ :\ \sqrt{J_{x_{top}}}-(\frac{a}{2})\sqrt{J_{\theta_{top}}}\le 0.02h$$

$$g_y\ :\ \sqrt{J_{y_{top}}}+(\frac{b}{2})\sqrt{J_{\theta_{top}}}\le 0.02h$$

$$k_{x_i}\ :\left|e_{x_i}\right|\le\frac{a}{2}$$

$$k_{y_i}\ :\left|e_{y_i}\right|\le\frac{b}{2}$$

$$i=1,2,...,n$$

As it can be seen the state variables are the vector of eccentricities (e) and frequency ratio (Γ_x). g_x, g_y , k_{x_i} and k_{y_i} are inequality constraints, a and b are the lengths of each floor in x- and y-direction respectively, n is the number of floors and h is the height of the structure.

5.2 Optimization Problem Solver

When the degrees of freedom are two the number of state variables in mathematical programming of (5.25) would be three (two eccentricities and the frequency ratio). This problem can be easily solved using the Optimization Toolbox of MATLAB. When the number of degrees of freedom increases, the optimization problem of (5.25) becomes highly nonlinear and complicated. It was observed that for structural models with higher

degrees of freedom MATLAB is not able to find the optimum solution. Therefore, an optimization software called KNITRO (www.ziena.com) was utilized as the optimization problem solver.

KNITRO, short for "*N*onlinear *I*nterior point *T*rust *R*egion *O*ptimization" (the "*K*" is silent) is produced by Ziena Optimization, Inc.. KNITRO was introduced in 2001 as a derivative of academic research at Northwestern University, and has undergone continual improvements. It is a powerful and robust software package to solve large scale mathematical optimization problems.

KNITRO provides 3 state-of-the-art algorithms/solvers for solving optimization problems. Each algorithm addresses the full range of nonlinear optimization problems, and each is constructed for maximal large-scale efficiency (www.ziena.com). These three algorithms are as follows:

The first algorithm is *Interior-point Direct* which applies barrier techniques and directly factorizes the KKT matrix of the nonlinear system. It performs best on ill-conditioned problems.

The second algorithm is *Interior-point CG* algorithm that applies barrier techniques using the conjugate gradient method to solve KKT subproblems. It provides an alternative to the Interior-point Direct algorithm when the KKT factorization is impractical or inefficient to form.

The third algorithm is *Active Set* algorithm, which combines classical active set principles with a novel linear programming subproblem to rapidly discover the set of binding constraints. Its behavior is significantly different from Interior-point algorithms, and it converges precisely to the active set to provide highly accurate sensitivity

information.

KNITRO offers interface to MATLAB. Thus for the purpose of this research the KNITRO solver is incorporated with the MATLAB programs written for the previous sections and it turned out to be successful and robust in solving the optimization problem of (5.25).

5.3 Numerical Studies

The proposed procedure for computing the optimum eccentricity and frequency ratio is applied to a single story building and a multi story building. The models are analyzed using four ground motion PSD functions. The PSD functions are generated using Kanai-Tajimi (Equation (5.15)) formula. The characteristics of ground motions are presented in Table 5.1. In addition to that the PSD functions used for analysis are plotted in Figure 5.2.

Table 5.1 Characteristics of Ground Motions Used for Optimization

Case Number	Ground Frequency ω_g (rad/sec)	Ground Damping Ratio (ξ_g)
1	3	0.6
2	6	0.5
3	12	0.6
4	18	0.4

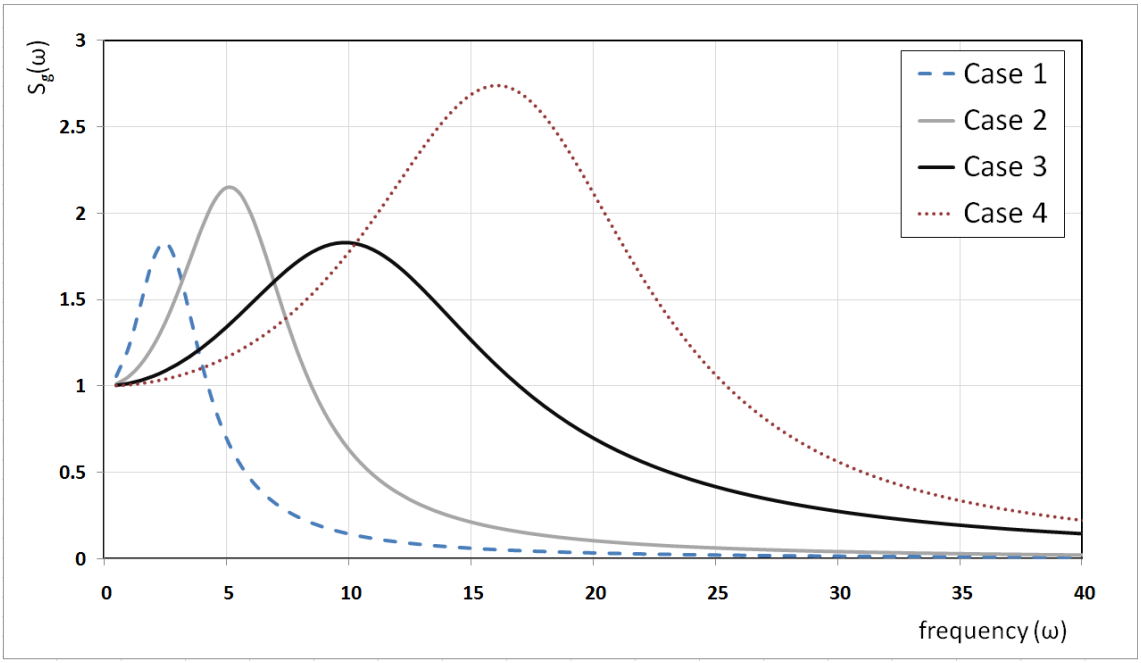

Figure 5.2 Kanai-Tajimi power spectral density functions of four ground motions used for optimization.

5.3.1 Single Story Building

Similar to previous chapters the first optimization problem to solve is finding the optimal eccentricity and frequency ratio of the single story building model shown in Figure (3.1). Since there is no eccentricity in *x*-direction the model has two degrees of freedom: one translational displacements and one rotation. The properties of the model are the same as in previous chapters; However, they are repeated herein for convenience.

The single story building model is basically a 24m×24m rectangular concrete slab. The mass of the floor is 203.04 metric tons and its height is about 3m. It is assumed that the translational frequency of the building is equal to 5.0 Hz in both directions. The damping of the model is assumed to be 3%.

The state (design) variables are the eccentricity and frequency ratio. In other

words values for eccentricity and frequency ratio are sought that minimizes the performance function of (5.16). The allowable eccentricity (e_{all}) is half of the floor dimension which is 12m. The allowable drift is considered to be 6 cm which is 2% of the model height.

The ground motions of Table 5.1 are applied to the single story building model and using KNITRO the constrained optimization problem of (5.25) is solved. After finding the optimal eccentricities and frequency ratios the minimized objective function is evaluated. Then its value is compared with performance function of a non-eccentric model with the same frequency ratio and the amount of reduction in performance function is computed. The results of this analysis are presented in Table 5.2.

Table 5.2 Optimal Eccentricity and Frequency Ratio (Single Story Building Model)

Ground Motion			Optimal Eccentricity* (%)	Optimal Frequency Ratio (Γ_x)	Reduction in Performance Function (%)
Case No.	ω_g (rad/sec)	ξ_g			
1	3	0.6	11.25	1.06	20.0
2	6	0.5	11.75	1.06	23.1
3	12	0.6	12.93	1.08	33.1
4	18	0.4	11.95	1.08	31.7

* Optimal eccentricities are presented as percentage of allowable eccentricity.

According to the above table the reductions are in a range of 20% to 33% which is significant. In addition to that the optimal eccentricities are fairly small and practical. They cover a range from 11% to 13% of allowable eccentricity. The frequency ratios are interestingly close to one. It is important to bear in mind that since the rotational constraints are not violated, all of the above reductions are achieved while the expected value of rotation is remained within the limits allowed by the codes.

Another interesting point that can be observed from Table 5.2 is the fact that for

the single story building studied, since the variation of optimal eccentricities and frequency ratios are close for all the ground motion cases, the optimal parameters are showing little sensitivity to the ground motion characteristics.

Furthermore the ground motion of Case 3 is applied to the non-eccentric and eccentric single story building with optimal parameters and the PSD functions are evaluated. These two PSD functions are compared in Figure 5.3. The effectiveness of eccentricity can be seen in Figure 5.3 where the translational displacement of the model is drastically supressed as the eccentricity is applied. The amount of reduction in the PSD function is about 66%.

Additionally Figure 5.3 could be a good explanation of how the idea of eccentricity works. The non-eccentric structure has one degree of freedom. By applying eccentricity another degree of freedom i.e. rotation is introduced. That is the reason that the PSDF of the eccentric structure has two peaks while the non-eccentric structure has only one. As it can be seen the overall response of eccentric structure is smaller than non-eccentric one. This could be explained in this way, which is the basic idea behind this research : in the non-eccentric model with one mode, the input energy leads to vibration in one direction, while for the eccentric model it is divided between two types (or modes) of vibration i.e. translational and rotational. Therefore, the translational response of the eccentric structure would be smaller than non-eccentric.

The time history of the translational displacement of the structure with and without optimal eccentricity is illustrated in Figure 5.4. For this purpose El Centro record (NS 1940) whose properties are very close to that of Case 3 is used. Good reduction in strucutral response has been achieved when the parameters of the eccentric

model are adopted through the proposed optimal desigh procedure. It can be seen that at the time when the maximum displacement of non-eccentric building occurs, the displacement of the eccentric model is interstingly very small.

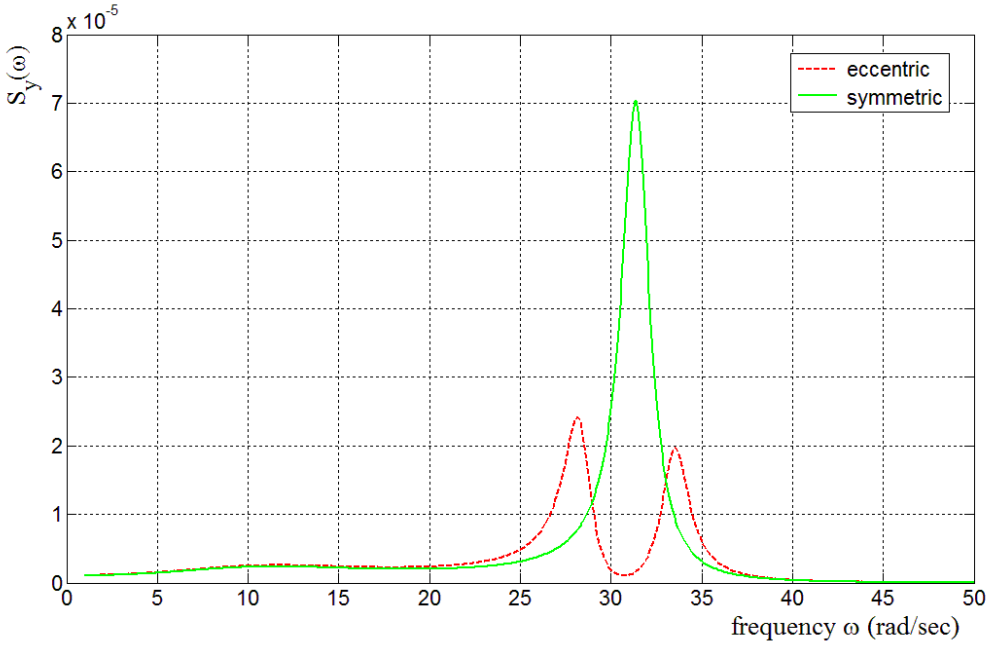

Figure 5.3 Comparison between the PSDF of translational response of optimal eccentric model and corresponding non-eccentric model.

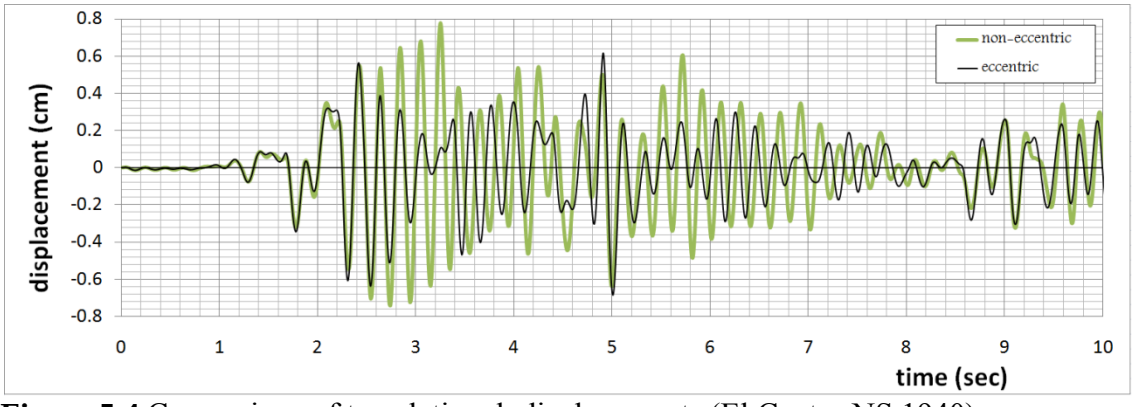

Figure 5.4 Comparison of translational displacements (El Centro NS 1940).

5.3.2 Multi-Story Building

The multi-story building is basically the stack up of 10 single story buildings of the previous section. Therefore, the dimensions of the floor slabs are 24 m × 24 m. The mass of each floor is 203.04 metric tons and the height of the structure is assumed to be 30 m. The stiffness of all the floors is assumed to be equal and it is determined in a way that the first (dominant) translational frequency of the structure is equal to 1.0 Hz in both directions. The damping of the model is 3%. The system is excited by the ground motions presented in Table 5.1.

The parameters to be optimized are the eccentricities at each floor and the frequency ratio of the structure. It is assumed that the eccentricities of each floor are equal in both *x*- and *y*-directions. The optimization problem is solved with two different assumptions. First it is assumed that eccentricity is constant over the height. In other words the same eccentricity is applied at each floor. Then for a separate analysis the optimization is performed assuming eccentricity can be variable over the height. In this case the optimal distribution of eccentricity over the height is sought.

The maximum allowable eccentricity is half of the floor length, which is equal to 12 meter. The maximum allowable top floor displacement is 2% of the building height and therefore is equal to 0.6 meter.

The results of optimization are shown in Table 5.3. This table basically presents the amount of reduction that can be achieved using the approach proposed in this chapter. Table 5.3 shows that the minimum reduction achieved is 37.40% and the maximum reduction can be as large as 50.43%.

Table 5.3 Optimal eccentricity and frequency ratio (10 story building model)

Ground Motion			Variable Eccentricity		Constant Eccentricity	
Case No.	ω_g (rad/sec)	ξ_g	Optimal Frequency Ratio (Γ_x)	Performance Function Reduction(%)	Optimal Frequency Ratio (Γ_x)	Performance Function Reduction(%)
1	3	0.6	1.17	43.48	1.17	40.23
2	6	0.5	1.06	37.34	1.06	35.30
3	12	0.6	1.04	45.10	1.05	43.02
4	18	0.4	1.06	50.43	1.07	48.27

Paying close attention to the results of Table 5.3 two interesting point is observed: first the results of optimization assuming variable eccentricity are very close to the results when eccentricity is assumed to be constant over the height. The second point is the fact that for the analysis performed herein the optimal frequency ratios are very close to each other and they are all in a small vicinity of one. A similar observation was made for the single story building as well.

The optimal distributions of eccentricity over the height of structure are illustrated in Figures 5.5 through 5.8. The optimal eccentricities when they are constant are plotted in the same graph too. Evaluation of Figures 5.5 to 5.8 reveals that the behavioral pattern of the optimal distribution of eccentricity is the same for all the cases studied. Evidently, the values of eccentricity in lower floors are smaller than middle and upper floors. Moreover the amounts of eccentricities are smaller than 30% of allowable value.

Additionally, Figures 5.5 to 5.8 show that the value of optimal constant eccentricity is very close to the optimal eccentricity of fifth floor when it is variable over the height. As a matter of fact the eccentricities of the top five floors are closer to the optimum constant eccentricity and their variations are smaller when compared to the bottom five floors of the building.

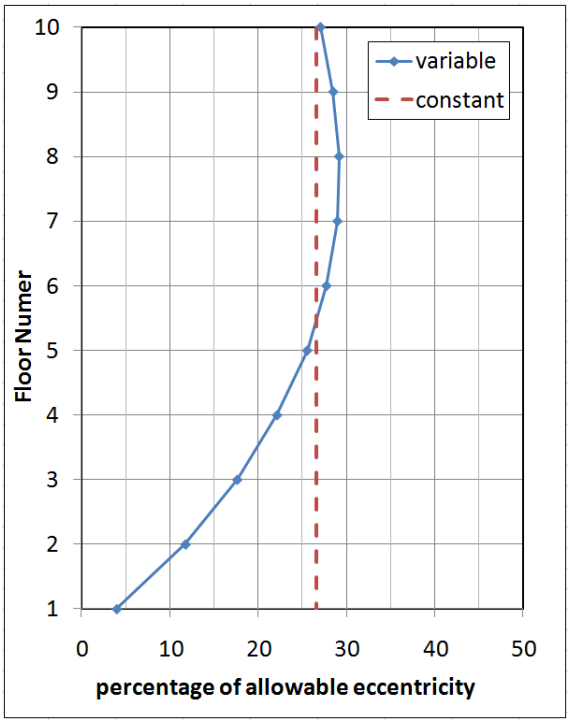

Figure 5.5 Optimal distribution of eccentricity over the height for a 10 story building (Ground motion Case 1).

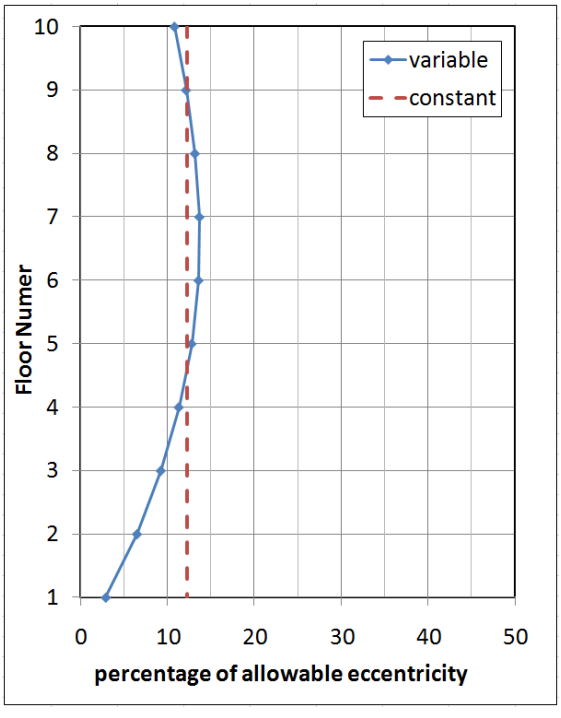

Figure 5.6 Optimal distribution of eccentricity over the height for a 10 story building (Ground motion Case 2).

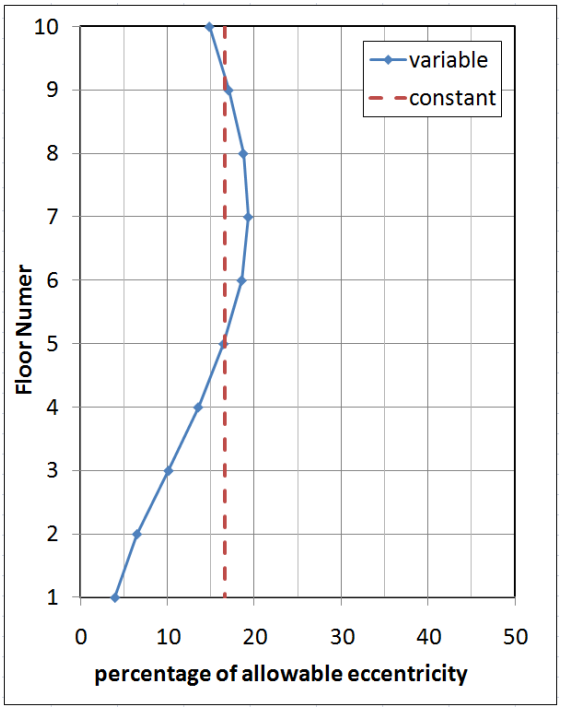

Figure 5.7 Optimal distribution of eccentricity over the height for a 10 story building (Ground motion Case 3).

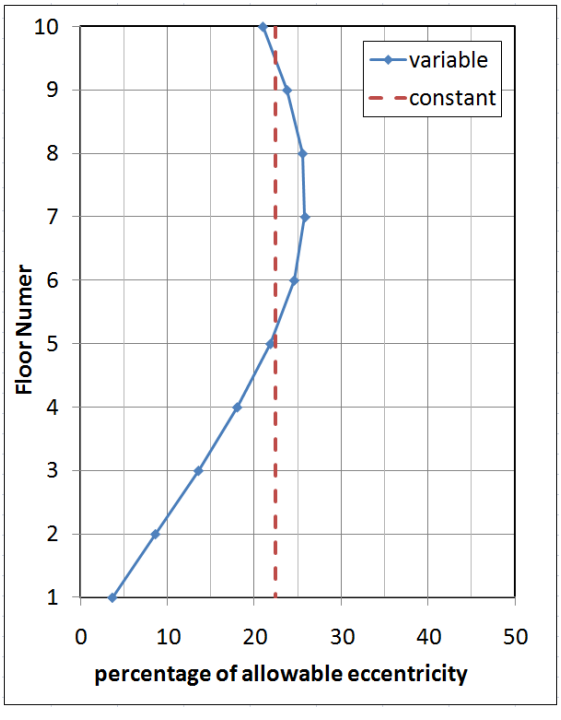

Figure 5.8 Optimal distribution of eccentricity over the height for a 10 story building (Ground motion Case 4).

In order to further investigate the optimal constant eccentricity and optimal distribution of eccentricity, the minimized performance functions for different ground motions are plotted in Figure 5.9. As it can be seen the minimized performance functions are very close and practically equal. This fact along with the fairly small value for optimal eccentricity (less than 30%) makes the eccentricities easier to accommodate for practical applications.

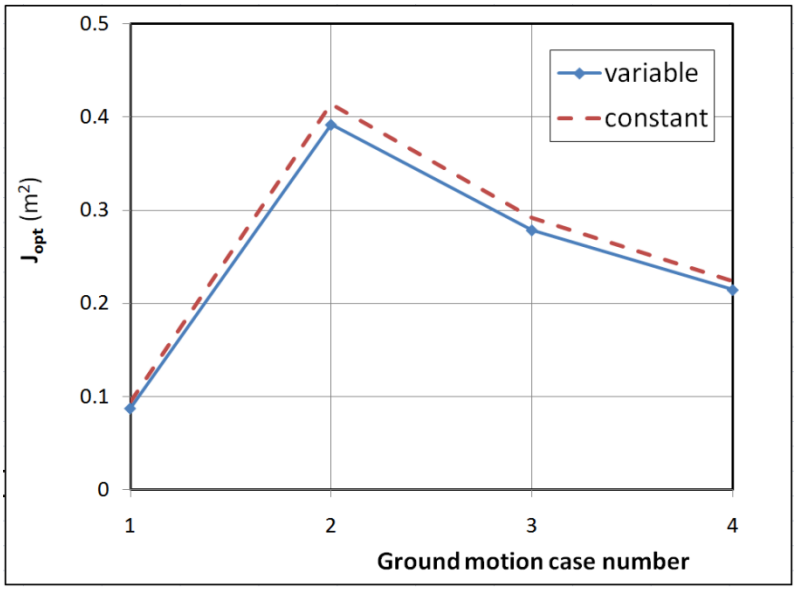

Figure 5.9 Comparison of optimum performance functions of the 10 story building with different distribution of optimal eccentricity.

Finally, a time history response of top floor of the structure with optimal eccentricity and frequency ratio are shown in Figure 5.10. The optimal parameters are taken from the optimization performed for Case 3. The eccentricity is assumed constant over the height. As it was mentioned earlier the ground motion properties of Case 3 are similar to that of El Centro NS 1940. Therefore, the time history of Figure 5.10 is produced by applying El Centro record to the 10 story building model. Figure 5.10 shows about 18.45% reduction in the maximum displacement of the eccentric structure.

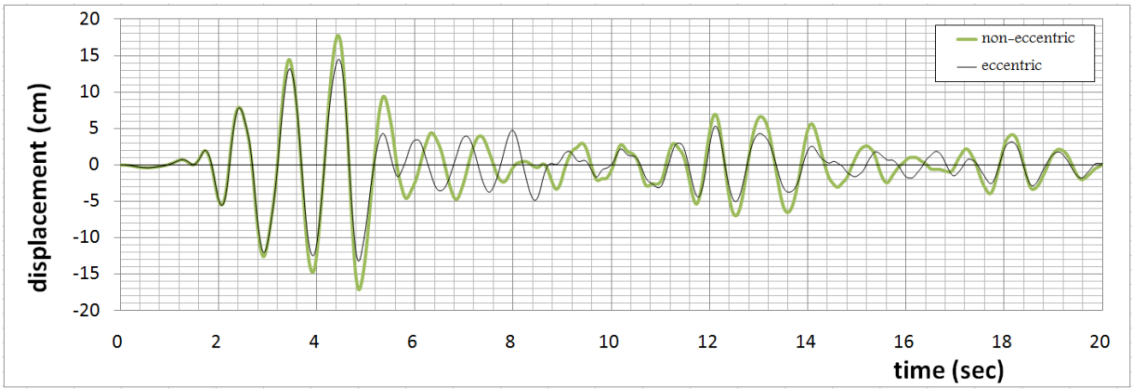

Figure 5.10 Top floor displacement responses of 10 story building with and without optimal eccentricity (El Centro NS 1940).

5.4 A Case Study

In an attempt to study the effectiveness of the proposed procedure, a model is selected from the literature. This model is among those for which the effectiveness of other control strategies has already been tested. The optimal eccentricity and frequency ratio according to the method proposed in this chapter are found and applied to the model. Then the reductions in displacements are compared.

For this purpose, a simplified model of a tall building is selected. This model was originally used by Feng and Mita (Feng and Mita 1995) to study the performance of their proposed vibration control system. Their system takes advantage of the mega-substructure configuration used in the design of tall buildings. In this system the mega-subcontrol system is designed in such a way that the vibration energy of the megastructure due to wind or earthquake loads can be transferred into the substructures and then dissipated in the substructures by conventional damping devices. In other words in this system the substructures in the mega-structure serve as vibration absorbers. Feng and Mita arrive at the parameters of the substructure by using a two-

degree-of-freedom system and minimizing the mean square response of the main mass to a white noise ground acceleration for seismic analysis and to a white noise force excitation for wind analysis.

The building equipped with the proposed mega-subcontrol system and its conventional counterpart without control system are shown in Figure 5.11. The two buildings have the same total mass to represent a 200 m tall building. The damping ratios are taken to be 2% for all vibration modes. The properties of the substructures computed according to Feng and Mita's method are presented in Table 5.4.

Sadek et al. (Sadek et al. 1997) have used the same structural model to demonstrate the effectiveness of their proposed method. Their method is based on defining a criterion to find the optimal design parameters of tuned mass dampers (TMD). The criterion they used to obtain the optimum parameters is to select, for a given mass ratio, the frequency (tuning) and damping ratios that would result in equal and large modal damping in the first two modes of vibration. They considered each substructure shown in Figure 5.11 as a separate tuned mass damper and using their proposed procedure they computed the optimal stiffness and damping. The optimal parameters of substructures calculated by Sadek et al. are shown in Table 5.4.

For the purpose of this research the building of Figure 5.11(a) was selected. It was modeled as a four-story-building for which the dynamic properties is the same in both *x*- and *y*-direction. The allowable eccentricity was taken to be 15 m. The ground motion properties were the same as Case 3 of Table 5.3, which is very close to El Centro (1940 NS) record. Using the procedure introduced in this chapter the optimal distribution of eccentricity and frequency ratio are found. Additionally the optimal

eccentricity and frequency ratio when eccentricity is assumed to be constant are obtained as well. The optimal distribution of eccentricity and optimal constant eccentricity and frequency ratios are presented in Table 5.5.

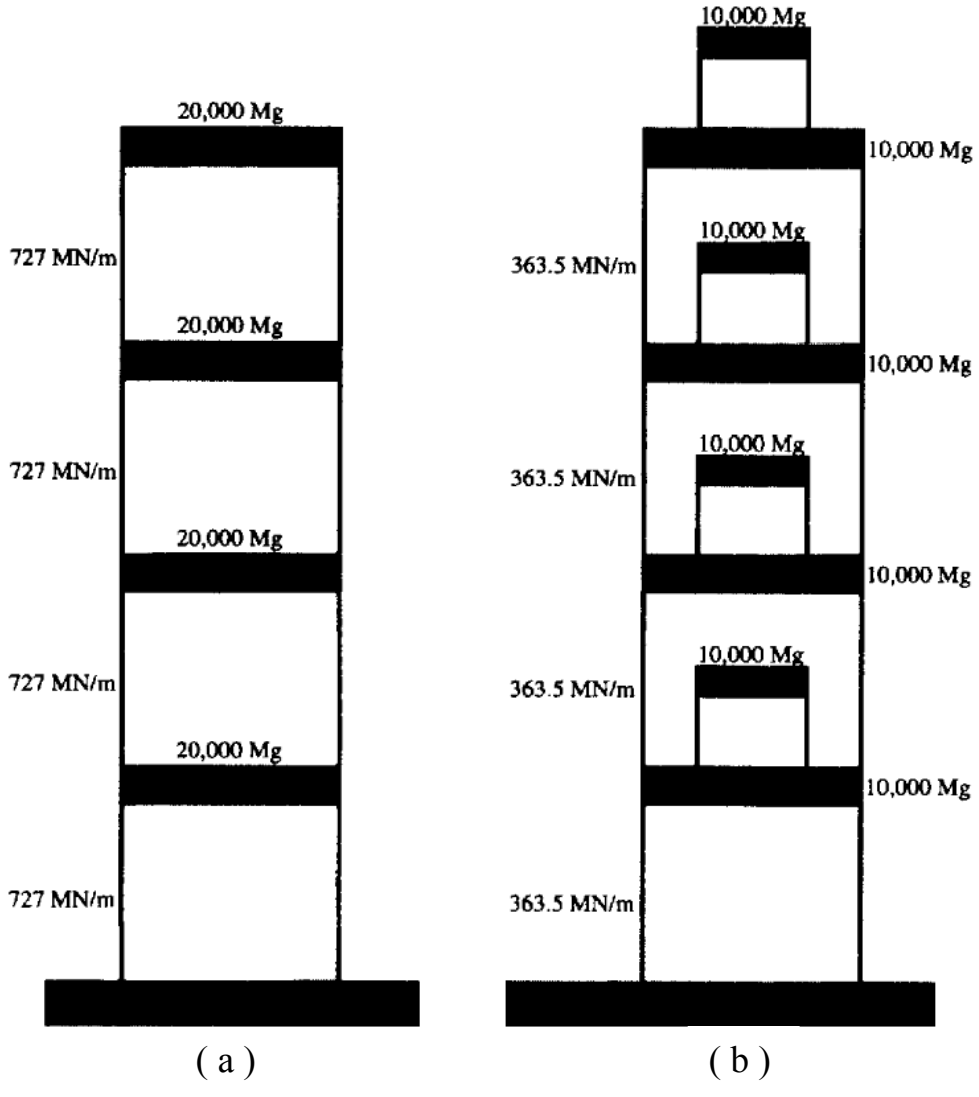

Figure 5.11 (a) Building without control. (b) Building with mega Sub-control.

Table 5.4 Optimal Properties of Substructures

Level	Feng and Mita's system		Sadek et. al's procedure	
	Stiffness (k) (kN/m)	Damping (c) (kN.s/m)	Stiffness (k) (kN/m)	Damping (c) (kN.s/m)
Top	5,480	6,411	23,655	18,452
3	5,480	6,411	25,233	16,756
2	5,480	6,411	28,638	13,249
1	5,480	6,411	34,457	7,733

Table 5.5 Optimal Eccentricities and Frequency Ratio

Level	Variable Eccentricity		Constant Eccentricity	
	Eccentricity (m)	Frequency Ratio (Γx)	Eccentricity (m)	Frequency Ratio (Γx)
Top	2.29	0.130	1.0	0.216
3	2.36			
2	1.92			
1	1.07			

Feng and Mita and Sadek et al. subjected the structure with optimal parameters to El Centro (1940 NS) record and compared the peak values with uncontrolled case. The peak values of displacement are compared in Table 5.6.

In concurrence with Feng and Mita and Sadek et al. work, the structure with optimal distribution of eccentricity is analyzed under El Centro (1940 NS) ground motion. The peak values of displacement are shown in Table 5.6.

Table 5.6 Peak Value of Displacements Under El Centro Record

Level	No Control	Feng and Mita*		Sadek et. al		Proposed Procedure
	Mega-Structure	Mega-Structure	Substructure	Mega-Structure	Substructure	Mega-Structure
Top	0.358	0.156	0.195	0.105	0.074	0.178
3	0.319			0.102	0.09	0.156
2	0.215			0.091	0.12	0.120
1	0.122			0.055	0.16	0.074

* Responses of lower stories not reported.

As it is evident from Table 5.5 all the control methods result in a considerable reduction in displacements. Sadek et al.'s method results in 70.7% reduction in displacement of top floor of the mega-structure. Feng and Mita's approach has reduced the displacement of top floor of mega-structure and substructure by 56.4% and 45.5% respectively. The approach proposed in this chapter mitigates the translational displacement of the top floor by 50.2%. This amount of reduction is significant and is comparable with the values achieved using other control strategies. Especially, it should be noted that the reduction achieved using this method is larger than the amount achieved by Feng and Mita for the substructure. This shows that using the proposed method even further reductions can be achieved compared to that reported by Feng and Mita. A comparison of time histories of top floor of mega-structure for controlled (eccentric) and uncontrolled (non-eccentric) case is illustrated in Figure 5.12. It is evident that the top floor displacement of eccentric structure is significantly smaller than non-eccentric. However, the frequencies of the two structure are very close. The relatively small value of the optimal eccentricity can be the reason.

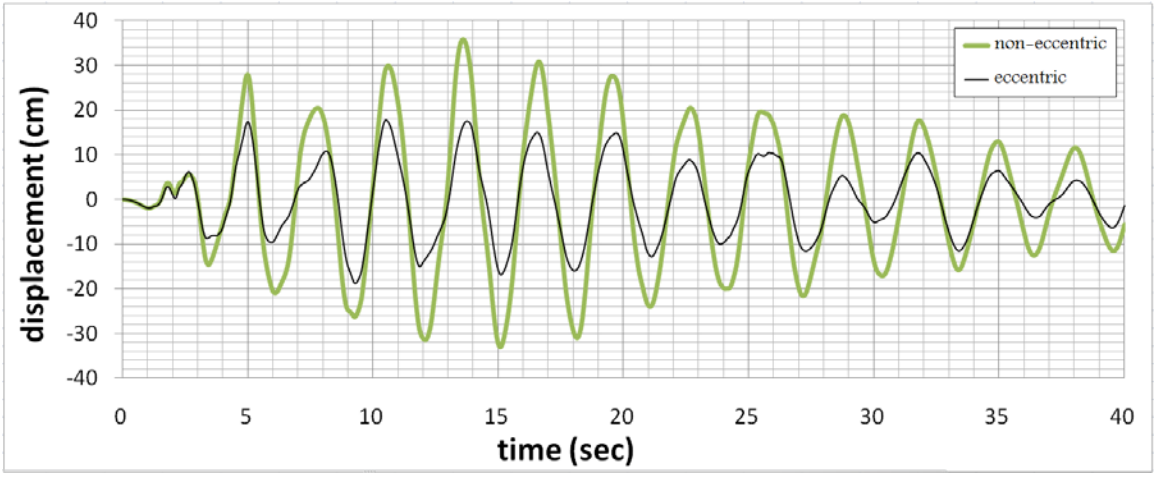

Figure 5.12 Comparison between time histories of top floor of mega-structure in controlled(eccentric) and uncontrolled(non-eccentric) cases.

CHAPTER 6

CONCLUSION

6.1 Summary

The objective of this thesis was developing a theory to engineer mass/stiffness eccentricity for structural motion control purposes. Four types of structural models were selected to study: single story building, multi story building, flexural beam and shear beam. It is expected that these four models cover a wide range of structural behavior.

First a steady state analysis was performed on the structural models. The main purpose of this analysis was to conduct an exploratory investigation of parameters that affect the response mitigation. Then through a statistical analysis the seismic effectiveness of engineered mass/stiffness eccentricity for structural control was studied. For this purpose 16 real earthquake records representing a wide range of frequency contents were selected. Then by changing the eccentricity and also the ratio of translational frequency to rotational frequency (called frequency ratio) in the models the effectiveness of the proposed idea for seismic application was confirmed. The steady state analysis and seismic statistical analysis turned out to be useful in providing a better understanding of the parameters that impact the performance of the proposed idea. Once the impact of different parameters in response control was examined the focus turned to devise a systematic approach to design these parameters for maximum vibration reduction.

To this end by combining basic concepts of control theory and random vibrations an optimization problem was formulated. In the optimization process the ground motion

was modeled using the well known Kanai-Tajimi ground power spectral density function. The objective function was the mean value of the squared displacements. Two types of constraints were included as well. First due to physical limitation an upper bound was imposed on eccentricity. Additionally, rotations generated by introducing eccentricity were constrained. Using an optimization program called KNITRO several numerical studies performed for a single story building and a multistory building. Finally through a case study the performance of the proposed method was compared with two other methods used for the same structure.

6.2 Conclusion

Based on the results of this study and analyses the following general conclusions were obtained:

- The results of both steady state analysis and statistical seismic analysis confirm that eccentricity of mass/stiffness can be effective in mitigation of translational vibration of structures.
- The steady state analysis of different structural models indicates that other than the amount of eccentricity the relationship between translational frequency and rotational frequency plays an important role in the level of response reduction. As far as steady state response of single story building is concerned, a necessary and sufficient condition (Equation (3.14)) was found under which increasing the eccentricity always leads to suppression of translational response. In addition to that it was observed that under this circumstances there is an eccentricity for which the translational displacement of center of mass diminishes.

- Statistical seismic analysis of structural models showed that application of eccentricity can lead to a substantial mitigation of translational response. The average amount of reduction achieved under 16 real earthquake records was from 20% to 30%. The closeness of mean and median value as well as fairly small values of standard deviation (20%) showed that for different earthquake records and structural properties the amount of reductions were clustered closely around the mean value.
- Statistical seismic analysis reveals that when frequency ratio is smaller than one the average of response reduction in single story building, multi story building and flexural beam is immensely sensitive to the response ratio. On the other hand the response ratio of the mentioned models show little sensitivity to frequency ratio for values of greater than one. This statement does not hold to be true for the shear beam model. Shear beam model has a moderate sensitivity for all values of frequency ratio.
- Statistical analysis confirms existence of optimal eccentricity. Optimal eccentricity is an eccentricity for which the maximum reduction in response is achieved.
- The comparison between time history analysis of eccentric and non-eccentric model shows that the time at which the maximum displacement occurs is not necessary the same for those two models. In other word introduction of eccentricity to the symmetric model not only changes the frequency of the structure but also alters the time at which the model experiences the maximum displacement.
- The proposed method for finding the optimal distribution of eccentricity and frequency ratio was used to select the optimal parameters of a single story building, multi-story building, flexural beam and shear beam. The results indicate that using the

proposed approach reduces the performance function, which is the mean value of squared displacements, significantly (up to 50%).

- The method was also compared with two vibration control systems proposed by Feng and Mita and Sadek et. al for tall buildings. It was observed that the level of reductions obtained using the proposed method is comparable with other control strategies. In some cases, once the proposed method is used, even further reductions can be achieved.

6.3 Recommendations For Further Study

This research was the first step towards providing a theoretical background for the idea of application of engineered mass/stiffness eccentricity in structural control, proposed by MacBain and Spillers in 2004. As the continuation of this work the following studies could be helpful in further development of this research:

- This dissertation was an attempt to provide a theoretical background for application of eccentricity in structural motion control. Therefore, the structural models used herein were mathematical models that solely provide general information about the behavior of structures. It is recommended that using more realistic models and analyses the findings of this thesis be further studied and investigated. For instance different types of structures could be modeled using Finite Element Programs and by conducting different linear and nonlinear analyses the translational response, when eccentricity is applied, could be studied. This type of analysis could be very informative with respect to performance of the proposed idea for practical applications.

- The objective of this work was studying the effect of eccentricity on translational displacements. However, for a control strategy to be successful, there are other parameters that need close attention. Two other parameters that were not studied in this work are accelerations and forces. Thus investigating the effect of eccentricity on accelerations and base shear are natural continuation of this research.
- As it was discussed earlier, to solve the optimization problem of Chapter 5, a computer program called KNITRO was utilized. KNITRO is a program designed to solve a broad range of optimization problems with different characteristics. However, while it proved to be powerful in finding the optimum points, the running time of some of the examples was very high. Thus it is recommended that a new optimization algorithm be designed that can solve the introduced optimization problems robustly with less computation cost.

REFERENCES

Abrate, S. (1995). Vibration of non-uniform rods and beams. *Journal of Sound and Vibration*, 185(4), 703-716.

ASCE (2005). *ASCE-7-05 Minimum Design Loads for Buildings and Other Structures*. Virginia: American Society of Civil Engineers.

Chen, G. & J. Wu (2001). Optimal placement of multiple tune mass dampers for seismic structures. *Journal of Structural Engineering*. 127(9), 1054-1062.

Chopra, A. K. (2006). *Dynamics of Structures.* New Jersey: Prentice Hall.

De Stefano, M. & B. Pintucchi (2008). A review of research on seismic behavior of irregular building structures since 2002. *Bulletin of Earthquake Engineering***,** 6(2), 285-308.

Dorf, R. & R. Bishop (2008). *Modern Control Systems*. New Jersey: Prentice Hall.

Feng, M. & A. Mita (1995). Vibration Control of Tall Buildings Using Mega-Sub Configuration. *ASCE Journal of Engineering Mechanics*, 121(10), 1082-1088.

Hoang, N., Y. Fujino, & Warnitchai, P. (2008). Optimal tuned mass damper for seismic applications and practical design formulas. *Engineering Structures*, 30(3), 707-715.

Hoang, N. & P. Warnitchai (2005). Design of multiple tuned mass dampers by using a numerical optimizer. *Earthquake Engineering & Structural Dynamics*, 34(2), 125-144.

Kanai, K. (1957). Semi-empirical formula for the seismic characteristics of the ground. *Bulletin of the Earthquake Research Institute*, 35, 309-325.

Lee, C., Y. Chen, Chung, L.L. & Wang, Y.P. (2006). Optimal design theories and applications of tuned mass dampers. *Engineering Structures*, 28(1), 43-53.

Li, C. & Y. Liu (2004). Ground motion dominant frequency effect on the design of multiple tuned mass dampers. *Journal of Earthquake Engineering*, 8(1), 89-105.

MacBain, K. & W. R. Spillers (2004). Exploring the use of three-dimensional dispersion to damp building vibrations. *Journal of Engineering Mechanics*, 130(3), 312-319.

Miranda, E. & Taghavi, S. (2005). Approximate Floor Acceleration Demands in Multistory Buildings. I: Formulation. *Journal of Structural Engineering*, 131(2), 203-211.

Ogata, K. (1996). *Modern Control Engineering.* New Jersey: Prentice-Hall Inc.

Sadek, F., Mohraz, B., Taylor, A.W., & Chung R.M. (1997). A method of estimating the parameters of tuned mass dampers for seismic applications. *Earthquake Engineering & Structural Dynamics*, 26(6): 617-635.

Spencer Jr, B. & Nagarajaiah S. (2003). State of the Art of Structural Control. *Journal of Structural Engineering*, 129(7), 845-856.

Tajimi, H. (1960). A statistical method of determining the maximum response of a building structure during an earthquake. *Proceedings 2nd World Conference on Earthquake Engineering*, II, 781-798.